LAWRENCE
LIVERMORE
NATIONAL
LABORATORY

LLNL-BOOK-816633

Chapter 1 Introduction to Surfactants

Y. Zhu, M. L. Free

November 10, 2020

Surfactants in Precision Cleaning

Disclaimer

This document was prepared as an account of work sponsored by an agency of the United States government. Neither the United States government nor Lawrence Livermore National Security, LLC, nor any of their employees makes any warranty, expressed or implied, or assumes any legal liability or responsibility for the accuracy, completeness, or usefulness of any information, apparatus, product, or process disclosed, or represents that its use would not infringe privately owned rights. Reference herein to any specific commercial product, process, or service by trade name, trademark, manufacturer, or otherwise does not necessarily constitute or imply its endorsement, recommendation, or favoring by the United States government or Lawrence Livermore National Security, LLC. The views and opinions of authors expressed herein do not necessarily state or reflect those of the United States government or Lawrence Livermore National Security, LLC, and shall not be used for advertising or product endorsement purposes.

SURFACTANTS IN PRECISION CLEANING

REMOVAL OF CONTAMINANTS AT THE MICRO AND NANOSCALE

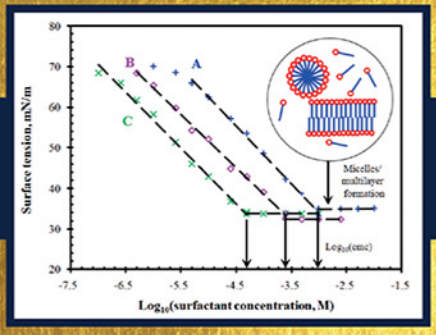

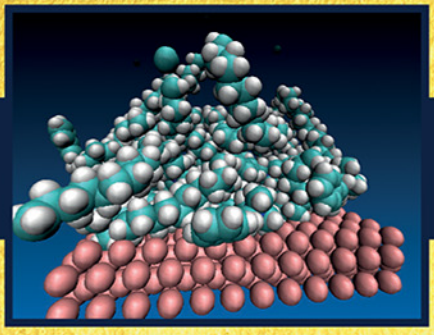

EDITED BY

RAJIV KOHLI

K. L. MITTAL

ELSEVIER

Surfactants in Precision Cleaning

Removal of Contaminants at the Micro and Nanoscale

This page intentionally left blank

Surfactants in Precision Cleaning

Removal of Contaminants at the Micro and Nanoscale

Edited by

Rajiv Kohli and K. L. Mittal

ELSEVIER

Elsevier
Radarweg 29, PO Box 211, 1000 AE Amsterdam, Netherlands
The Boulevard, Langford Lane, Kidlington, Oxford OX5 1GB, United Kingdom
50 Hampshire Street, 5th Floor, Cambridge, MA 02139, United States

Copyright © 2022 Elsevier Inc. All rights reserved.

No part of this publication may be reproduced or transmitted in any form or by any means, electronic or mechanical, including photocopying, recording, or any information storage and retrieval system, without permission in writing from the publisher. Details on how to seek permission, further information about the Publisher's permissions policies and our arrangements with organizations such as the Copyright Clearance Center and the Copyright Licensing Agency, can be found at our website: www.elsevier.com/permissions.

This book and the individual contributions contained in it are protected under copyright by the Publisher (other than as may be noted herein).

Notices
Knowledge and best practice in this field are constantly changing. As new research and experience broaden our understanding, changes in research methods, professional practices, or medical treatment may become necessary.

Practitioners and researchers must always rely on their own experience and knowledge in evaluating and using any information, methods, compounds, or experiments described herein. In using such information or methods they should be mindful of their own safety and the safety of others, including parties for whom they have a professional responsibility.

To the fullest extent of the law, neither the Publisher nor the authors, contributors, or editors, assume any liability for any injury and/or damage to persons or property as a matter of products liability, negligence or otherwise, or from any use or operation of any methods, products, instructions, or ideas contained in the material herein.

British Library Cataloguing-in-Publication Data
A catalogue record for this book is available from the British Library

Library of Congress Cataloging-in-Publication Data
A catalog record for this book is available from the Library of Congress

ISBN: 978-0-12-822216-4

For Information on all Elsevier publications
visit our website at https://www.elsevier.com/books-and-journals

Publisher: Matthew Deans
Acquisitions Editor: Christina Gifford
Editorial Project Manager: Mariana Kühl Leme
Production Project Managers: Prasanna Kalyanaraman
Melissa Read
Cover Designer: Matthew Limbert

Typeset by MPS Limited, Chennai, India

Contents

This page intentionally left blank

List of Contributors

Daksh Agrawal Lam Research Corporation, Fremont, CA, United States

Aravindha Antoniswamy Materials Science and Engineering, University of Texas at Austin, Austin, TX, United States

Nadia F. Awad Ultrasonic Apps LLC, Pearland, TX, United States

Sami B. Awad Ultrasonic Apps LLC, Pearland, TX, United States

Rajesh Balachandran Micron Technology Inc., Boise, ID, United States

Nikhil Dole Lam Research Corporation, Fremont, CA, United States

Michael L. Free Department of Materials Science & Engineering, University of Utah, Salt Lake City, UT, United States

Manish Keswani Materials Science and Engineering, University of Arizona, Tucson, AZ, United States

Rajiv Kohli The Aerospace Corporation, NASA Johnson Space Center, Houston, TX, United States

Jatinder Kumar Applied Materials, Santa Clara, CA, United States

Malcolm McLaughlin Alconox Inc., White Plains, NY, United States

Michael Moussourakis Alconox Inc., White Plains, NY, United States

Jin-Goo Park Department of Materials Science and Chemical Engineering, Hanyang University, Ansan, Republic of Korea

Jeff Phillips Alconox Inc., White Plains, NY, United States

Maneesh Kumar Poddar Department of Chemical Engineering, National Institute of Technology Karnataka, Surathkal, India

Endu Sekhar Srinadhu Lam Research Corporation, Fremont, CA, United States

Vikhram V. Swaminathan Lam Research Corporation, Fremont, CA, United States

Dinesh P.R. Thanu Materials Science and Engineering, University of Arizona, Tucson, AZ, United States

Nagendra Prasad Yerriboina Department of Materials Science and Chemical Engineering, Hanyang University, Ansan, Republic of Korea

Mingrui Zhao Applied Materials, Santa Clara, CA, United States

Yakun Zhu Department of Materials Science & Engineering, University of Utah, Salt Lake City, UT, United States; Materials Science Division, Lawrence Livermore National Laboratory, Livermore, CA, United States

This page intentionally left blank

About the Editors

Dr. Rajiv Kohli is a leading expert with The Aerospace Corporation in contaminant particle behavior, surface cleaning, and contamination control. At the NASA Johnson Space Center in Houston, Texas, he provides technical support for contamination control related to ground-based and manned spaceflight hardware, as well as for unmanned spacecraft. His technical interests are, in particle, behavior, precision cleaning, solution and surface chemistry, advanced materials, and chemical thermodynamics. He was involved in developing solvent-based cleaning applications for use in the nuclear industry and also developed an innovative microabrasive system for a wide variety of precision cleaning and microprocessing applications in the commercial industry. He is the senior editor of the 12-volume book series *Developments in Surface Contamination and Cleaning*, published from 2008 to 2019. Previously, he coauthored the book *Commercial Utilization of Space: An International Comparison of Framework Conditions* and published more than 300 technical papers, articles, and reports on precision cleaning, advanced materials, chemical thermodynamics, environmental degradation of materials, and technical and economic assessment of emerging technologies. He was recognized for his contributions to NASA's Space Shuttle Return to Flight effort with the Public Service Medal, one of the agency's highest awards.

Dr. Kashmiri Lal "Kash" Mittal was associated with IBM from 1972 to 1994. Currently, he is teaching and consulting in the areas of surface contamination and cleaning and adhesion science and technology. He is the founding editor of the new journal *Reviews of Adhesion and Adhesives* that made its debut in 2013. He cofounded the *Journal of Adhesion Science and Technology* and was its Editor-in-Chief until April 2012. He is the editor of

more than 140 published books, many of which deal with surface contamination and cleaning. He was recognized for his contributions and accomplishments by the worldwide adhesion community that organized in his honor on his 50th birthday, the First International Congress on Adhesion Science and Technology in Amsterdam in 1995. The Kash Mittal Award was inaugurated in his honor for his extensive efforts and significant contributions in the field of colloid and interface chemistry. Among his numerous awards, he was awarded the title of doctor *honoris causa* by the Maria Curie-Skłodowska University in Lublin, Poland, in 2003. In 2014 two books entitled *Recent Advances in Adhesion Science and Technology* and *Surfactants Science and Technology: Retrospects and Prospects* were published in his honor.

Preface

Surfactants constitute an important and unique class of chemicals. These are used in a legion of processes and products for a myriad of purposes. In other languages, such as French, German, and Spanish, the word surfactant does not exist, and the actual term used to describe these substances is based on their propensity to lower the surface or interfacial tension, for example, tensioactif (French), tenside (German), and tensioactivo (Spanish).

Surfactants possess dual characteristics, that is, hydrophilic and hydrophobic (lipophilic) portions. Surfactants essentially exhibit two main phenomena, adsorption and aggregation (e.g., micelles and other aggregated structures). Broadly speaking, surfactants are classified into four categories: anionic, cationic, nonionic, and zwitterionic.

The focus of this book is on precision cleaning using surfactants. Precision cleaning is described as cleaning to the desired level or better without introducing new contaminants. Both adsorption and aggregation behaviors of surfactants are important and relevant in removing various contaminants, such as particulates, organic films, ionic, and microbial contaminants, from a variety of surfaces. The individual contributions in this book provide state-of-the-art reviews by subject-matter experts on surfactants and their role in the removal of surface contaminants at the micro- and nanoscale.

The first chapter by **Yakun Zhu and Michael Free** is an introduction to surfactants and addresses the adsorption performance of a wide array of surfactants. Surfactant adsorption is driven by amphiphilic properties of surfactant as well as surface properties such as charge and composition. The hydrophilic–hydrophobic nature of surfactants results in interfacial adsorption and aggregation. Surfactants tend to form submonolayers, monolayer/hemimicelle, or bilayers/cylindrical micelle structures at interfaces and surfaces. The concentration needed to achieve monolayer coverage is usually close to the cmc for the surfactant. Aggregation of surfactant above the cmc leads to the formation of spherical micelles and other structures. These structures act like a buffer that maintains the free monomeric surfactant concentration constant when the total surfactant concentration exceeds the level needed for micelle formation. The free monomeric surfactant concentration determines the level of adsorption on a surface. It is possible to predict surfactant adsorption based on material properties, surfactant properties such as

hydrocarbon chain length, and solution conditions such as pH and ionic strength. There are several challenges to more accurate fundamental modeling and predictions of surfactant adsorption, aggregation, and partitioning which are discussed by the authors.

Contaminants on surfaces can be in many forms and may be present in a variety of states on the surface and have detrimental impacts on the performance of products. Their removal is essential for all processes where the surface must be aesthetically or functionally modified, such as bonding, deposition of thin films and protective coatings, or surface patterning. The objective of the chapter by **Rajiv Kohli** is to provide a good understanding of the nature of surface contaminants and the cleanliness levels of surfaces that are fundamental to the development of methods for the removal of contaminants from surfaces. The use of surfactants is a well-established method to aid in removal of surface contaminants at the micro and nanoscale and is the focus of the present book. The most common categories of surface contaminants are particles, thin film or molecular contamination that can be organic or inorganic, ionic contamination, and microbiological contamination. The sources of contaminants and mechanisms of their generation are discussed that can assist in developing remediation solutions.

Surfactants can enhance particle removal from surfaces by modifying the particle−surface interaction forces. In their second chapter, **Michael Free and Yakun Zhu** discuss how adsorbed surfactant molecules can alter the van der Waals attractive force, electrostatic force, hydrophobic force, as well as provide a steric barrier to contact. The effect of surfactants on these forces can result in greatly enhanced particle removal efficiency. Surfactant adsorption density and structure are important factors in determining removal enhancement performance associated with surfactants. Cleaning is generally most effective above the surface aggregation concentration (sac), which for naturally hydrophilic surfaces allows for bilayer or multilayer level surfactant coverage that provides significant charge repulsion as well as a steric barrier. Adsorption below the monolayer level renders naturally hydrophilic substrates hydrophobic, which tends to reduce removal efficiency. In contrast, naturally hydrophobic surfaces are likely to benefit from both submonolayer and multilayer coverages of surfactants that occur, respectively, below and above the sac. Existing adsorption theory and available formulas can aid in the prediction of the sac, which is an important parameter in predicting the performance of surfactants in particle removal enhancement. Equations are available to predict the effectiveness of surfactants in enhancing particle removal.

Semiconductor manufacturing involves several processing steps, where cleaning is critical before and after each processing step. **Nagendra Prasad Yerriboina, Maneesh Kumar Poddar and Jin-Goo Park** discuss two major wet processing steps in silicon wafer cleaning and post-CMP (chemical mechanical planarization) cleaning that requires a higher level of cleaning to obtain a contamination-free surface. Depending on the application,

different physical and chemical forces are used. Surfactants are critical during semiconductor cleaning to remove the particles during different processing steps. The primary mechanism involved in removing particles by surfactants is to weaken the particle adhesion to the substrate and adsorb onto the particle surface and substrate, creating either steric forces or repulsive forces. One of the challenges is to remove particles from patterned surfaces. The coupling of surfactants with megasonics would be very effective in enhancing PRE (particle removal efficiency) and reducing pattern damage. Contamination by the slurry particles is the major concern after the CMP process. Hence, a proper cleaning solution in combination with poly(vinyl acetate) brush scrubbing is used. Surfactants are very critical in removing the particles from Si, oxide, metal, and III−V material surfaces. As discussed in their chapter, various mechanisms are involved in removing the slurry particles from these surfaces and play an important role in Si wafer cleaning in controlling the etch rates by adsorbing on the wafer surface.

Particulate contamination remains a major issue for yield loss in semiconductor manufacturing as integrated circuit (IC) companies are facing a constant challenge in continuing miniaturization for device structure and configuration. The requirements for semiconductor cleaning are becoming more and more stringent as new materials are being introduced in advanced technology node that has reduced feature size and has increased aspect ratio, while pushing for higher PRE to maintain or increase the yield. One of the multiple challenges that the semiconductor industry is facing in maintaining the current scaling trends is the removal of undesired contamination, typically originating from the environment or fabrication process steps. **Dinesh Thanu, Aravindha Antoniswamy, Vikhram Swaminathan, Endu Sekhar Srinadhu, Nikhil Dole, Mingrui Zhao, Rajesh Balachandran, Daksh Agrawal, Jatinder Kumar, and Manish Keswani** address acoustic cleaning as a type of noncontact cleaning method that utilizes sound waves through a liquid medium to remove particulate contaminants from surfaces by applying physical forces to separate particles from substrates. This technique can be easily implemented and has been employed as a preferred alternative in IC industries compared to aggressive chemical cleaning for years. Surfactants are commonly used as additives in cleaning formulations during acoustic cleaning of semiconductor surfaces. Since surfactants are surface active, they can affect cavitation characteristics and, thereby, influence cleaning efficiency and damage to the surface. Cleaning steps are among the most critical since they are repeated several times during microelectronic fabrication. In particular, the critical size of the particles to be removed has decreased, following the general IC aggressive scaling trends, to below 30 nm. Hence, surfactants can be effective tools in modulating the interaction forces between the surface and contaminants, and in acoustic cavitation in cleaning during wafer fabrication.

The chapter by **Sami Awad and Nadia Awad** is focused on ultrasonics in precision cleaning. The fundamental mechanisms and advantages and

issues involved in ultrasonic cleaning, as well as cleaning chemistry are described for different kinds of contaminants. Surfactants play an important role in ultrasonic cleaning as illustrated by several examples of challenging industrial applications, including aqueous removal of submicrometer and nanometer-size particles, semiaqueous cleaning of tough to clean greases and heavy oils, and aqueous cleaning of steels with full protection from flash rusting. The authors also discuss the prospects of the technology.

Critical cleaning denotes situations in which the level of cleaning directly impacts the value of the end product or manufacturing efficiency. In their chapter, **Malcolm McLaughlin, Michael Moussourakis and Jeff Phillips** describe how choosing a surfactant or aqueous detergent for a critical cleaning application requires careful selection of cleaning chemistry and methods to ensure adequate performance without sacrificing worker or environmental safety. The authors group aqueous detergent selection criteria into three broad categories: function and efficacy, health and safety, and environmental, as well as provide selected application examples illustrating the effectiveness of the detergents. Once an aqueous detergent or detergent group is selected, cleaning validation is necessary to confirm the reproducibility and reliability of the process. Each cleaning validation study specifies a particular detergent and method used for cleaning, as well as the product being manufactured, potential contaminating residue, and equipment used for manufacturing. There is no one-size-fits-all solution to cleaning validation studies—any individual validation will depend on the industry, manufacturer, manufactured product, equipment, cleaning concern, and contamination potential, among other factors. The cleaning validation process is reviewed in detail, and specific recommendations and guidance for the key industries of pharmaceutical and medical device manufacturing are provided.

We would like to express our heartfelt thanks to all the authors in this book for their contributions, enthusiasm, and cooperation. Our sincere appreciation goes to our publishers Mariana Kühl Leme, Christina Gifford, and Matthew Deans, who have strongly supported the publication of this volume. Melissa Read and the editorial staff at Elsevier have been instrumental in seeing the book to publication. Swapna Praveen was very helpful with copyright permissions for use of the figures. Rajiv Kohli would also like to thank the staff of the STI library at the Johnson Space Center for their efforts in helping to locate obscure and difficult-to-access reference materials.

Rajiv Kohli
Houston, TX, United States

K. L. Mittal
Hopewell Junction, NY, United States

Chapter 1

Introduction to Surfactants

Yakun Zhu[1,2] and Michael L. Free[2]

[1]*Materials Science Division, Lawrence Livermore National Laboratory, Livermore, CA, United States,* [2]*Department of Materials Science & Engineering, University of Utah, Salt Lake City, UT, United States*

Chapter Outline

1 Introduction

A group of widely used organic molecules are surfactants, sometimes referred to as tensioactive chemicals or tensides, which usually consists of hydrophilic and hydrophobic molecular sections [1–6]. The amphiphilic nature of surfactant molecules creates an affinity for adsorption at interfaces such as the metal/metal oxide–water interface. The properties of surfactants and the interaction of surfactants with metal or metal oxide and the surrounding solution environment determine the level of adsorption. Understanding the behavior of surfactants is critical to optimal utilization of surfactants in adsorption on a metal/metal oxide surface, aggregation and partitioning in aqueous and/or organic phase, as well as the applications of surfactants in areas such as particle removal, pharmacy, and cosmetics.

Surfactants in Precision Cleaning. DOI: https://doi.org/10.1016/B978-0-12-822216-4.00003-3
© 2022 Elsevier Inc. All rights reserved.

Surfactants are generally categorized into four different groups according to the nature of their head groups: anionic (A), cationic (C), nonionic (N), and zwitterionic (Z) (see example in Table 1.1). As indicated by their names, anionic and cationic surfactants are charged, and a counterion of opposite charge is attached to the head group to keep charge neutrality; metal cations are typical counterions for anionic surfactants and halogen ions are common counterions for cationic surfactants. Nonionic surfactants have no charge associated with their head group, whereas zwitterionic surfactants are characterized by having two distinct and opposite charges (positive and negative) on the molecule at either adjacent or nonadjacent sites. Another term, amphoteric, is often used, which is a subset of zwitterionic surfactants; these surfactants have a charge that depends on pH. One example of a class of surfactant molecules is the homologous benzalkonium chlorides (BACs), alternatively named hexadecyltrimethylammonium bromide (C_{16}, $C_{16}Cl$, or $C_{16}BzCl$), as shown in Fig. 1.1A and B. C_{16} has an N-based aromatic functional group that is hydrophilic, and a hydrophobic hydrocarbon tail with 16 linear CH_2 and CH_3 sections. The hydrophilic group strongly prefers interaction with polar entities such as water or other ions, whereas the hydrophobic section strongly prefers interaction with other hydrophobic entities such as hydrocarbons. This dual nature of surfactants determines their interactions with surfaces and interfaces. The information of all the surfactant compounds discussed in this chapter is summarized in Table 1.1.

2 Hydrophilicity and Hydrophobicity of Surfactant Molecules

The hydrophilic functional group of surfactant molecules strongly prefers interaction with polar entities such as water, metals, and other ions. Generally, surfactants adsorb on the metal surface, block the active sites such as those surfaces exposed to corrosive media, and thereby reduce corrosion attack [6–11]. It is believed that the structure of heterocyclic surfactant molecules plays a dominant role in the surfactant adsorption. The presence and structure of specific atoms, such as N and O, in these molecules strongly influences the adsorption mechanism [6–11].

The hydrophobic portion, which is nonpolar, strongly prefers interaction with hydrophobic entities such as hydrocarbon phase [6,11,12]. Therefore surfactant molecules are prone to adsorb at and cover the surfaces/interfaces, such as air–liquid surfaces and liquid–solid interfaces, to escape from polar solvents such as water by associating and packing hydrocarbon chains together. The surfactant concentration at which a monolayer of surfactant molecules adsorbs on and covers a metal surface is termed the surface aggregation concentration (sac) [4–6,10,11,13–16]. As surfactant concentration increases, bilayers/multilayers are likely to form on surfaces. Surfactant molecules can also form aggregates in aqueous phase at solubility saturation in a way that they usually orient their hydrophobic tails toward those of neighboring surfactant molecules and their

TABLE 1.1 Name, Structure, Symbol, and Chain Length (*n*) of Surfactants (Symbols are used in the text for the Corresponding Surfactants).

Surfactant Name	Structure	Symbol	*n*	Type
n-[2-[(2-aminoethyl) amino] ethyl]-9-octadecenamide	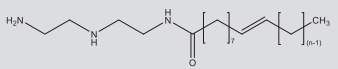	AAOA	8	N
n-Benzalkonium chloride	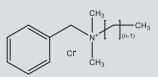	C_n, C_nCl, or C_nBzCl	12, 14, 16	C
$C_nH_{(2n+1)}$-COO$(CH_2CH_2O)_{12}CH_3$	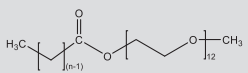	C_nCOOE_{12}	9	N
Polyoxyethylene alkyl ether	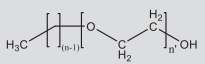	$C_nE_{n'}$	12, 16	N
n-Alkyltrimethylammonium surfactant	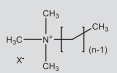	C_nTAX (X = Br^-, Cl^-)	10, 12, 14, 16	C
Potassium alkanoate	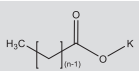	$C_nH_{(2n+1)}KO_2$	9, 11	N
Dodecylpyridinium bromide	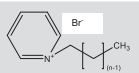	DDPB	12	C
Octylglucoside	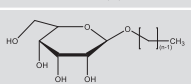	OG	8	N

(*Continued*)

TABLE 1.1 (Continued)

Surfactant Name	Structure	Symbol	*n*	Type
Sodium dodecyl sulfate	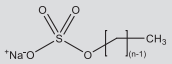	SDS	12	A
Trans-cinnamaldehyde	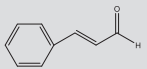	TCA	–	N
Sodium bis-(2-ethylhexyl)-sulfosuccinate	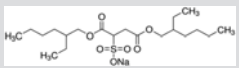	AOT	–	A
Cetylpyridinium chloride	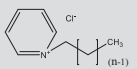	CPC	14	C
Primary alcohol ethoxylate	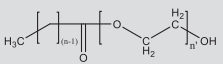	CnOEn′	11	N
Polyoxyethylene nonyl phenyl ether	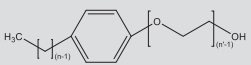	NPEn′	9	N
Poly(ethylene glycol) esters	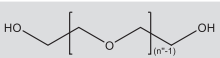	–	–	N
Linoleate		–	–	N
Dodecylamine		DDA	11	N

N-based alkyl amines and derivatives		$CnNH_2$	6	N
		$C_nN(CH_3)_2$	4	N
	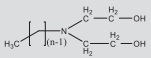	$C_nN(CH_2CH_2OH)_2$	6	N
		C_nNO	4	N
	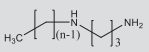	$C_nNH(CH_2)_3NH_2$	10	N
3-[(3-Cholamidopropyl)dimethylammonio]-1-propanesulfonate	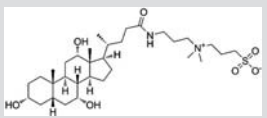	CHAPS	–	Z
Cocamidopropyl hydroxysultaine	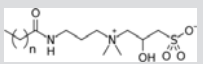	CAHS	6, 8, 10, 12, 14, 16	Z

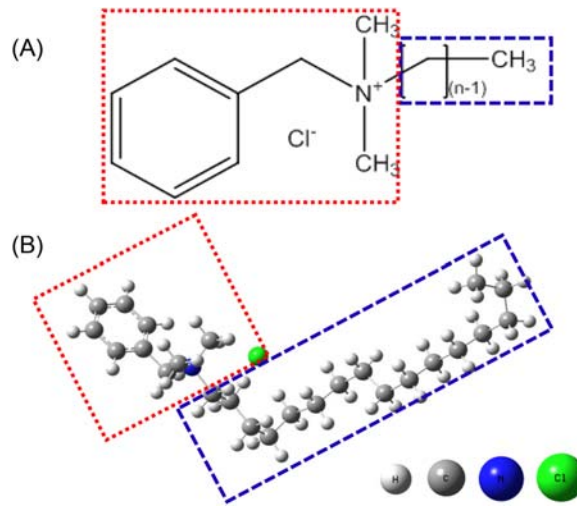

FIGURE 1.1 Chemical formula of benzyldimethylhexadecylammonium chloride (C_{16}, or $C_{16}Cl$, or $C_{16}BzCl$) (A) and the corresponding optimized molecular geometry (B).

hydrophilic head groups toward water or hydrophilic surfaces. The surfactant concentration at which surfactant molecules start to form aggregates such as micelles in solution is termed the critical micelle concentration (cmc) [4–6,10,11,13–16]. It has been shown that the sac is usually much lower than the cmc and that high efficiency of surface coverage is usually achieved at the sac provided that the surfactant is a good adsorbate [6,11,13].

Hydrophilic–lipophilic balance (HLB) is the measure of the size and strength of the hydrophilic and hydrophobic moieties of a surfactant molecule. The HLB concept, proposed by Griffin in 1949 [17], is the best-known semiempirical method to select a surfactant suitable for an application. In this semiempirical method a surfactant is assigned an HLB number according to its chemical structure. The HLB number ranges from 0 to 20 and depending on the scale, surfactants can be classified for different applications (Table 1.2) [18].

Metal and metal oxide surfaces are hydrophilic [19]. Consequently, the functional group in surfactant molecules is attracted to surfaces of metals and metal oxides. The attraction to surfaces is strengthened by the hydrophobic portion of the molecule that is attracted to other hydrophobic portions of adjacent surfactant molecules on surfaces. Thus there is a driving force for surfactant adsorption on metal and metal oxide surfaces that orients the surfactant with the hydrophilic group at the solid surface and the hydrophobic hydrocarbon chain directed out into the solution, thereby creating a hydrophobic surface. This driving force causes surfactant molecules to aggregate on surfaces. If sufficient surfactant is present in solution, a second layer or multiple layers of surfactant may adsorb creating a variety of adsorbed

TABLE 1.2 Hydrophilic–Lipophilic Balance (HLB) Scale Showing Classification of Surfactant Applications.

Compatibility With Water/Oil	Applications	HLB
Oil-soluble HLB < 10	Antifoaming agents	1–3
	W/O emulsifying agents	3–6
	Wetting and spreading agents	7–9
Water-soluble HLB > 10	O/W emulsifying agents	8–16
	Detergents	13–15
	Solubilizing agents	15–18

O, Oil; *W*, water.

structures. Surfactants behave in a similar way in solution with aggregate structures such as micelles forming at moderate concentration levels above the cmc [20].

It is usually assumed that surfactant adsorption or surface coverage in the presence of low surfactant concentration (usually lower than the micelle formation concentration) can be represented by the number of active surface sites of substrate covered by surfactant adsorption [4,6,21–23]. More and more active surface area is covered by surfactants as surfactant concentration increases. Near the sac and the cmc, the surface is assumed to be covered by one monolayer and multilayers/micelles of surfactants, respectively [4,6,21–23]. Surfactants form micelles at solubility saturation in the aqueous phase. The surfactant may form reversed micelles in the oil phase at a certain concentration that is termed the oil cmc (Γ^{o}). The cmc in aqueous phase is termed the aqueous cmc (Γ^{w}). The overall average concentration at which the micelle starts to form in the oil–water binary phase environment is termed the apparent cmc (Γ^{ap}).

3 Adsorption Mechanism

The surfactant adsorption mechanism is usually determined by the adsorption free energy ΔG^{o}_{ad}, which is correlated to the adsorption constant using the following equation [6,24]:

$$K_{ad} = \frac{1}{C_{mw}} \exp\left(-\frac{\Delta G^{o}_{ad}}{RT}\right) \tag{1.1}$$

where K_{ad} is the equilibrium adsorption constant, which is usually calculated based on various adsorption isotherms that will be discussed in

Section 12.2; C_{mw} is molar concentration of water, which is 55.5 M; and R is the gas constant, and T is absolute temperature.

Generally, a negative value of ΔG^{o}_{ad} signifies that the adsorption of surfactant on a metal surface is a spontaneous process and shows a strong interaction between surfactant molecules and hydrophilic surfaces with appropriate bonding sites such as steel [25,26]. If ΔG^{o}_{ad} is more positive than −20 kJ/mol, the interaction between surfactant and a surface is often classified as physisorption due to electrostatic interaction. When ΔG^{o}_{ad} is more negative than −40 kJ/mol, the adsorption usually involves charge sharing or transfer between the surfactant molecules and the surface to form coordination bonds, which is also classified as chemisorption [26,27]. However, physisorption can sometimes be energetically favorable and significant, whereas chemisorption may sometimes have relatively weak binding energy due to various factors that influence adsorption [27,28].

Because chemisorption involves a chemical reaction between the adsorbate and the surface to form a specific bond, it is generally limited to a monolayer. In contrast, physisorption does not have a specific bonding requirement and can involve multiple layers under some conditions. The high bonding energy associated with chemisorption often requires elevated temperature or exposure of concentrated competitive ions to desorb chemisorbed molecules. Physisorbed molecules are readily desorbed at moderate temperatures or by lowering related vapor pressures or concentrations. Surfactant adsorption is related to surface tension, wettability, and other phenomena, and their influence has been studied in great detail [29–37].

4 Surface Tension

Surface tension occurs when cohesive energy exists between molecules. Hydrogen bonds and van der Waals interactions are present between water molecules in aqueous media. However, at the air–water interface, hydrogen bonds are not complete above the interface. Similarly, van der Waals interactions are weakened at the interface because there are no interacting molecules in the air phase. Therefore molecules present at the air–water interface have fewer bonding opportunities and greater available energy than those in the bulk phase. This excess energy is the basis for surface tension.

In aqueous media the hydrophobic portion of surfactant molecules has a tendency to move to available interfaces to escape the undesirable polar solvent. Adsorbed surfactant molecules at the air–water interface decrease surface tension. Thus surfactant molecules are more active at the air–water interface. Correspondingly, the term “surfactant” is derived from “surface-active agent” that lowers surface tension. Compounds that have higher cohesive energy at the air–water interface than that between water molecules are expected to increase surface tension.

Surface tension is related to the adsorption density as described mathematically in the Gibbs adsorption equation [38,39]:

$$\Lambda_i = -\left(\frac{1}{RT}\cdot\frac{d\mathrm{Y}}{d\ln a_i}\right)_{T,P} \tag{1.2}$$

where Λ_i is surface excess or adsorption density of surfactant i in number of molecules per unit area or in mol/m^2, Y is surface tension in force per unit length or in mN/m, and a_i is activity of surfactant i. The Gibbs adsorption equation shows that the adsorption density increases as the slope of surface tension versus the logarithm of concentration becomes steeper. Adsorption density, when multiplied by the effective thickness of the surfactant layer to obtain volumetric concentration units, indicates that the concentration of surfactant (solute) at the surface is higher than in the bulk. In the bulk solution, surfactant is dispersed and more dilute than at the interface where it is aggregated and packed more densely. Thus adsorption density is effectively the local concentration of surfactant at the adsorption interface.

The surface tension of solution decreases gradually as surfactant concentration increases until it reaches a minimum plateau value. As the interface becomes more packed, additional surfactant molecules tend to aggregate in solution as well as at solid−liquid interfaces. Additional surfactant above the level needed for minimum surface tension is utilized to form aggregate structures like micelles. The surfactant concentration needed to produce micelles is known as the cmc. The cmc generally represents the maximum concentration of surfactant monomers that can be dissolved in solution. The cmc is reached as the surface tension reaches the minimum plateau level. Because of this aggregation phenomenon occurring at the cmc, the Gibbs equation is not valid above the cmc. All surfactant in solution that is in excess of the cmc forms aggregate structures such as micelles and acts as a separate phase.

Fig. 1.2 shows surface tension data of BAC, including dodecyltrimethylammonium bromide C_{12} (or C_{12}Cl or C_{12}BzCl), tetradecyltrimethylammonium bromide C_{14} (or C_{14}Cl or C_{14}BzCl), and hexadecyltrimethylammonium bromide C_{16} (or C_{16}Cl or C_{16}BzCl), which can be used to determine the cmc [13]. As expressed in the Gibbs adsorption equation, the surface excess increases as water molecules are replaced by surfactant molecules at the surface provided that the surface tension versus $\log_{10}$(concentration) increases the magnitude of its slope. Usually the change in slope is large at low concentrations and then remains nearly constant as the cmc is approached.

The surface tension of water at the air−water interface at room temperature is 72 mN/m [40]. Appropriately selected hydrocarbon surfactants are usually able to decrease the surface tension to around 35 mN/m. Surfactants with fluorocarbon chain groups are capable of decreasing the surface tension to 25 mN/m [41]. Addition of a salt can further reduce surface tension due to

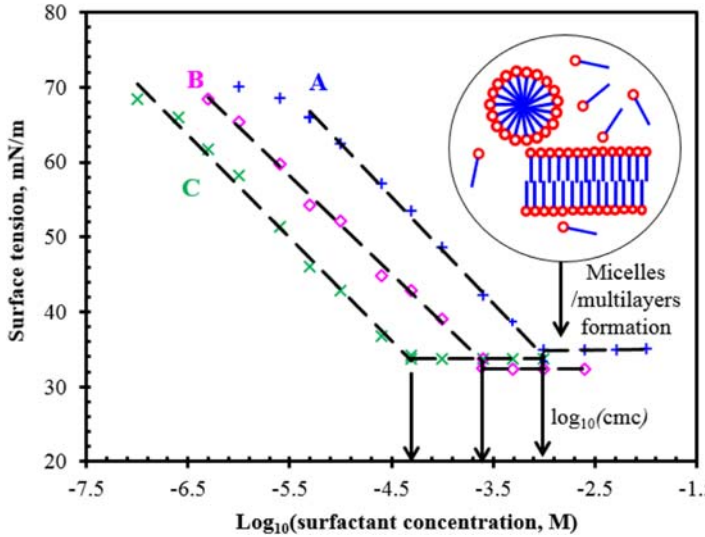

FIGURE 1.2 Plots of surface tension of aqueous solution as a function of surfactant concentration at 40°C: A—C_{12}BzCl in 0.171 M NaCl solution; B—C_{12}BzCl in 0.856 M NaCl solution; C—mixed C_{12}BzCl, C_{14}BzCl, and C_{16}BzCl at ratio of 0.15/0.70/0.15 in 0.171 M NaCl solution. The arrows pointing to *x* axis indicate the cmc values. The cmc is usually defined as the concentration where the decrease of surface tension stops or switches to a very low slope. The plots indicate what is likely occurring with respect to surfactant adsorption and aggregation as a function of surfactant concentration and surface tension. *cmc*, Critical micelle concentration.

decreased repulsion between ionic head groups of surfactant molecules that enhances molecular packing [42].

5 Enhancement of Wettability

The contact angle of a liquid droplet on a solid surface is the physical manifestation of the balance of three interfacial tension values as presented in Young's equation [43,44]:

$$\cos\Theta = \frac{Y_{SV} - Y_{SW}}{Y_{WV}} \tag{1.3}$$

where Y_{SO} is the interfacial tension of solid−vapor interface, Y_{WO} is the interfacial tension of water−vapor interface, Y_{SW} is the interfacial tension at the solid−water interface, and Θ is the contact angle of the liquid droplet on the solid surface. A representation of these interfacial tensions is presented in Fig. 1.3.

Young's equation indicates that a decrease in interfacial tension at the solid−water interface with the addition of surfactant results in a decrease in

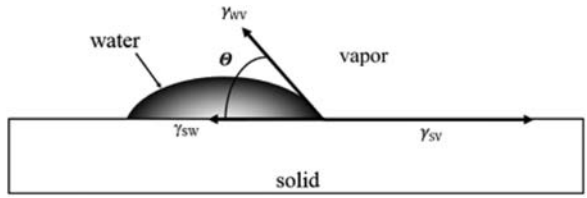

FIGURE 1.3 Illustration of contact angle of water in oil on a solid substrate.

the contact angle. A decrease in the contact angle is an indication of increased wettability. The ability of a liquid to spread or wet a surface is described mathematically using the spreading coefficient [45]:

$$\Delta Y = Y_{SV} - (Y_{SW} + Y_{WV}) \tag{1.4}$$

Wettability is controlled primarily by the hydrophilicity of the surface. Surfaces that are very hydrophilic have very low contact angles. The contact angle is a function of the surface tension as indicated in Young's equation. Surface tension is a thermodynamic property. Consequently, wettability is a thermodynamic result of the interactions of the associated phases. Wettability can be controlled by controlling the surface tension values through the use of surfactants as well as through selection of liquids and the solid interface.

Hydrophilic surfaces repel organic phases such as oils, and hydrophobic surfaces repel water. Consequently, when oil and water are mixed, the water in the mixture will attract to hydrophilic surfaces such as steel, precipitated salts, and corrosion product layers even though oil phases may be present. However, as the surfactant adsorbs on a surface, it can modify the wettability. In some cases, surfactants can change the character of a surface from one that is hydrophobic to one that is hydrophilic or from a hydrophilic surface to a hydrophobic surface.

Wettability can be affected by the surface roughness. Previous research shows wettability is affected by roughness as expressed by the relation [43,44]:

$$\cos\Theta' = f \cdot \frac{Y_S - Y_{SL}}{Y_L} = f \cdot \cos\Theta \tag{1.5}$$

where Θ' is the contact angle of a rough solid surface, f is a roughness factor that is greater than unity for rough surfaces, Y_S is surface tension of solid, Y_L is surface tension of liquid, and Y_{SL} is interfacial tension between solid and liquid. It is well-known that surface heterogeneity (contamination due to the presence of attached fine particles), thin films, deformation, and other phenomena can affect the contact angle [44]. Surfaces can be made exceptionally hydrophobic or "superhydrophobic" by creating microscale roughness on a normally hydrophobic surface [46].

6 Langmuir–Blodgett Films

Surface pressure, which is related to surface tension, and molecular surface area for monolayer films at the air–liquid interface are commonly measured and manipulated using a Langmuir–Blodgett (LB) balance [47]. The LB technique can be used to reveal interesting behavior of adsorbed surfactant molecules. The surface pressure of LB films, P_{LB}, is defined as [47,48]:

$$P_{LB} = Y_o - Y \tag{1.6}$$

where Y_o is surface tension without an adsorbed layer, and Y is the surface tension with an adsorbed layer. The LB balance can be used to measure surface pressure as the surface area of the adsorbed film is changed by surface compression using a movable barrier. Thus, the LB method can be used to modify the area occupied per surfactant molecule using a movable compression barrier.

When the surface pressure in an LB film device is low and the surface area per molecule is high, surfactant molecules are well dispersed and often are not oriented vertically at the interface. This well-dispersed molecular state is often related to the gas phase because of its resemblance to dispersed gas molecules. Multiplying the surface pressure by the surface area leads to the ideal gas equation analog for a two-dimensional surface [49]:

$$P_{LB}A_{LB} = n_{LB}RT \tag{1.7}$$

where A_{LB} is surface area of LB film and n_{LB} is the number of moles of adsorbed surfactants on LB film. As the LB surface area decreases, surfactant molecules become more close-packed, and the surface pressure increases. This often leads to a molecular state that is analogous to a liquid.

Further decrease in surface area forces tight molecular packing and the surface pressure reaches a maximum value. This tightly packed condition is analogous to a solid phase because the molecules are packed and can have two-dimensional, crystal-like structures. The LB film balance can be used to produce oriented multilayer films by transferring the films to substrates that are moved slowly through the air–water interface. Thus, the LB film balance can be used to transfer surfactant films of varying packing density as monolayers or multilayers to any solid substrate. Consequently, properties such as hydrophobicity and diffusion barrier performance can be evaluated using these films as a function of molecular packing and/or the number of multilayers on a substrate.

7 Krafft Point

Surfactant molecules do not dissolve appreciably in aqueous solutions below a certain temperature, known as the Krafft point [50]. Above the Krafft point

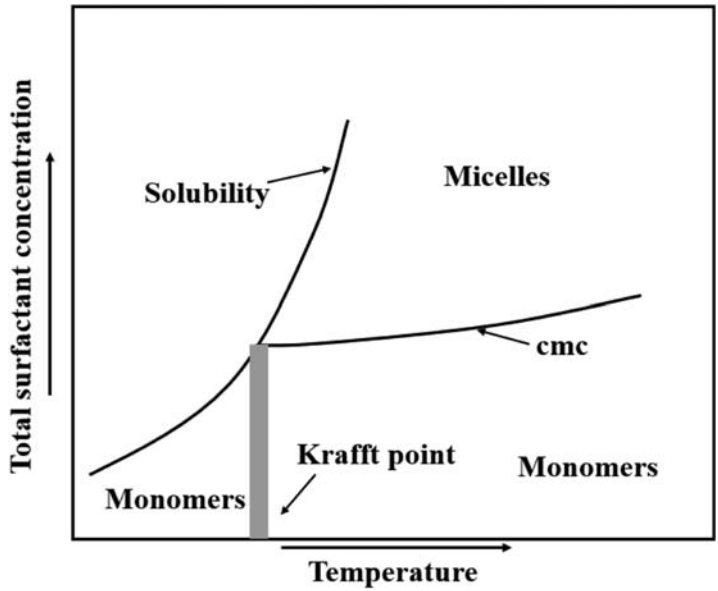

FIGURE 1.4 Comparison of total surfactant concentration and temperature and its relationship with surfactant states. Arrows next to the axes point toward the increasing direction.

or temperature, surfactants can form micelles, which greatly increases overall surfactant solubility. A diagram illustrating the relationship between the Krafft point and monomer and micelle surfactant forms is presented in Fig. 1.4. Thus, the Krafft point provides an important boundary condition for surfactant utilization.

8 Surfactant States

Surfactants can organize into different phases or states. The phase or state of surfactant is generally closely related to concentration. If surfactant concentration increases above the cmc, monomeric surfactants form aggregate structures such as micelles. Properties of micelles, the micellization process, and associated modeling will be discussed in detail in subsequent sections. The quantitative relationships amongst the total surfactant concentration, monomer concentration, micelle concentration, and the associated cmc are presented in Fig. 1.5. In addition to micelles, surfactants can form gels at the gel temperature [43,51]. Surfactants can also form liquid crystals. The gel state is the transition between the liquid crystal phase and the solid state. Surfactant in the gel state can change orientation and rotate. In contrast, surfactant dissolved in solution can have full freedom unless it is part of aggregate structures.

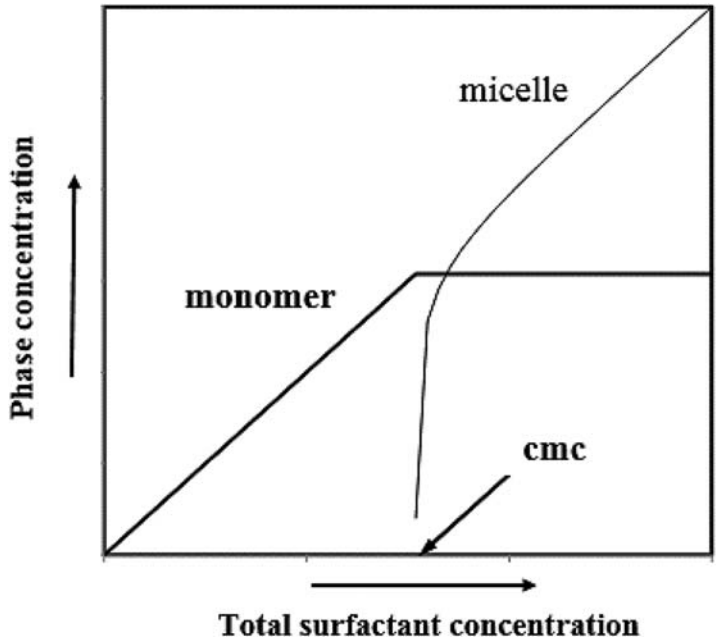

FIGURE 1.5 Comparison of phase (micelle or monomer) concentration and total surfactant concentration for a hypothetical surfactant. Arrows next to the axes point toward the increasing direction.

At elevated temperatures, some surfactants have decreased solubility. This decrease is due to reduced hydrogen bonding resulting from higher energy and conformational changes in surfactant structure that reduces bonding with water. Consequently, some surfactant solutions become cloudy at elevated temperatures due to the reduced solubility above the "cloud point" due to secondary phase formation. The cloud point effect is generally associated with nonionic surfactants.

9 Micelles

Surfactant molecules are compelled to aggregate to form micelle-like structures above the cmc. A micelle generally consists of tens to hundreds of surfactant molecules [28,52]. The number of surfactant monomers in a micelle is known as the aggregation number. The molecular weight of a micelle can be obtained simply by multiplying the aggregation number by the molecular weight of the surfactant monomer.

The aggregation number of surfactants is affected by ionic strength, head group properties, hydrophobic chain dimensions, and temperature. If there is a change in ionic strength of solution, the change can affect the aggregation

number. Increasing ionic strength weakens the repulsion between ionic head groups and increases the repulsion of the hydrophobic tail from the aqueous medium, thereby enhancing the tendency for aggregation. The head groups of surfactant molecules determine the size outside the hydrophobic micelle core. Small head groups facilitate aggregation. Temperature also influences aggregation [53]. Increasing temperature can cause surfactant to dehydrate the hydrophilic group of surfactants, which can result in increased hydrophobicity. However, increased temperature also decreases the tendency to adsorb at interfaces.

Micelles are constantly interacting and exchanging with individual surfactant molecules. Individual monomer surfactant molecules move in and out of micelles at the microsecond time scale [54]. In contrast, micelles form and dissociate at a time scale of milliseconds. However, these time scales change very significantly as the concentration of surfactant and the size and characteristics of the surfactant change.

Micelle aggregates form in shapes that include plate-like micelles, hemimicelles, spherical micelles, rod-like or cylindrical micelles, and vesicles [28,55]. The governing factor of the shape of a micelle is the packing of the hydrocarbon chain of the surfactant. Israelachvili showed a packing parameter (shape factor) will determine the tendency to form spherical micelles or nonspherical micelles [28]. The packing parameter $\boldsymbol{P_s}$ can be expressed as [28]:

$$\boldsymbol{P_s} = \frac{\boldsymbol{v_s}}{\boldsymbol{a_o l_s}} \tag{1.8}$$

where $\boldsymbol{v_s}$ is a hydrocarbon chain volume, $\boldsymbol{a_o}$ is an optimal surface area of surfactant head group, and $\boldsymbol{l_s}$ is a critical chain length. The preferred structure of micelles is summarized in Table 1.3 according to the packing parameter. A spherical micelle is shown in Fig. 1.6 along with the dimensions used for the packing factor [28].

TABLE 1.3 Micelle Structure as a Function of Packing Parameter P_s [28].

Value of Packing Parameter	Structure
$P_s \leq 1/3$	Spherical micelle
$1/3 < P_s < 1/2$	Ellipsoidal micelle
$P_s \approx 1/2$	Cylindrical micelle
$1/2 < P_s < 1$	Various interconnected structures
$P_s \approx 1$	Vesicles and extended bilayers
$P_s > 1$	"Inverted" structures

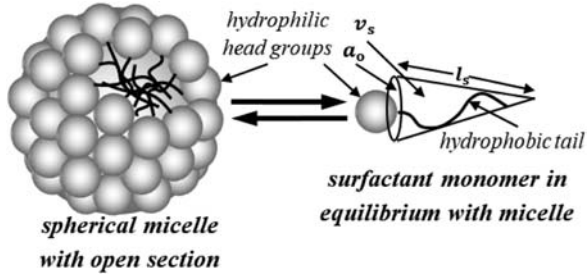

FIGURE 1.6 Spherical micelle in equilibrium with an individual surfactant monomer with associated parameters.

The aggregation number of a spherical micelle, N_{sph}, and the aggregation number per unit length of a cylindrical portion of the aggregate, N_{cyl}/l_s, are calculated from the aggregate radii r_{sph} and r_{cyl} [28]:

$$N_{sph} = \frac{4}{3}\frac{\pi r_{sph}^3}{v_s} \tag{1.9}$$

$$\frac{N_{cyl}}{l_s} = \frac{\pi r_{cyl}^2}{v_s} \tag{1.10}$$

r_{sph} and r_{cyl} are given, respectively, by [28]:

$$r_{sph} = \frac{3v_s}{a_o} \tag{1.11}$$

$$r_{cyl} = \frac{2v_s}{a_o} \tag{1.12}$$

The surface charge density of a spherical micelle and of a cylindrical portion is given by the following equation [56]:

$$\sigma_{sph} = \frac{q}{a_o}\left(\frac{r_{sph}}{r_{sph}+r_h}\right)^2 \tag{1.13}$$

$$\sigma_{cyl} = \frac{q}{a_o}\frac{r_{cyl}}{r_{cyl}+r_h} \tag{1.14}$$

where q is the charge of the head group of the surfactant and r_h is the distance from the location of the charge of head group to the surface of the micellar core. r_h is specific to the particular head group.

Tanford demonstrated that the critical chain length l_s and hydrocarbon chain volume can be approximated by the following equations [55]:

$$l_s \leq l_{max} \cong (0.154 + 0.1265L_i) \quad \text{nm} \tag{1.15}$$

and

$$v_s \cong (27.4 + 26.9L_i) \cdot 10^{-3} \quad \text{nm}^3 \tag{1.16}$$

where l_{max} is the maximum length of surfactant molecule and L_i is the number of carbon atoms in the hydrocarbon chain of surfactant i. Thus, the micelle packing parameter for DDPC (dodecylpyridinium chloride) with an aggregation number of 80 is 0.37 (>0.33). A value greater than 0.33 indicates the DDPC micelle is likely to be nonspherical.

Micelles are generally considered to be a separate liquid phase. Micelles behave as a separate phase from a thermodynamic perspective. Correspondingly, some compounds dissolve in micelle liquids [57,58]. Hydrophobic entities dissolve in the hydrophobic interior of micelles in aqueous solutions. In organic media where micelles are inverted with polar interiors, aqueous or polar entities are dissolved in the micelle interior.

10 Microemulsions

Microemulsions are similar to solutions with micelles. They consist effectively of swollen micelles that contain a 5- to 100-nm droplet of liquid inside. They can exist in an oil continuous phase with nanosized water droplets inside of a surfactant shell, or they can exist in a water continuous phase with oil droplets inside. Microemulsions, which have a wide variety of uses, consist of alcohol with an ionic surfactant as well as water and oil. Microemulsions can also be synthesized using water, oil, and a single surfactant such as sodium bis-(2-ethylhexyl)-sulfosuccinate, which is also known as AOT [59]. Microemulsions are thermodynamically stable forms of emulsions [60].

11 Surfactant Mixtures

In practical applications, surfactant mixtures have received wide attention because of their superior physicochemical properties and capabilities in efficient adsorption, solubilization, dispersion, suspension, and transportation [6,61,62]. Solutions containing mixed surfactants can often be conveniently tuned to achieve desired properties by adjusting the mixture composition. More surface-active and expensive surfactants are usually mixed with less surface-active and less expensive surfactants to reduce cost [6,11].

It is believed that there is a synergistic effect of mixed surfactants on adsorption and surface coverage of metals/metal oxides [6,11,26], which results in improved performance of mixed surfactants relative to pure surfactant. The synergistic adsorption has been shown to be an effective method of improving the adsorption efficiency, decreasing the amount of dosage, and diversifying the application of surfactants [6,11,26]. In addition, a cooperative effect in surface coverage of some surfaces occurs upon introduction of

halide ions to aqueous media. However, the addition of halide ions may either stimulate or inhibit surfactant adsorption, depending on the concentration. It has been reported that the inhibitive effects of halides follow the order of $I^- >> Br^- > Cl^-$. The strong synergistic effect of iodide ion can be explained by the chemisorption with some surfaces such as steel because of its larger size and polarizability [63,64].

A synergistic parameter, S_{sn}, is introduced to describe the combined surface coverage behavior of amines and halide ions given in the following [65]:

$$S_{sn} = \frac{1 - \theta_{1,2}^{calc}}{1 - \theta_{1,2}^{meas}} \tag{1.17}$$

where $\theta_{1,2}^{meas}$ is the experimentally measured surface coverage of mixed surfactants 1 and 2. $\theta_{1,2}^{calc}$ is the calculated surface coverage assuming no interaction between the surfactants and is given by the following equation:

$$\theta_{1,2}^{calc} = \theta_1 + \theta_2 - \theta_1\theta_2 \tag{1.18}$$

where θ_1 and θ_2 are surface coverages of surfactants 1 and 2, respectively. It is generally agreed that if S_{sn} approaches 1 no interaction between the two surfactants exists, if $S_{sn} > 1$ a synergistic effect applies, and that if $S_{sn} < 1$, an antagonistic interaction predominates [63–65].

Appropriately mixed surfactant systems have also been shown to improve the performance of some desirable interfacial properties. In a study by Shiao and coworkers [66], the effects of chain length matching of mixed surfactants on melting points, evaporation retardation, micellar stability, foaming, lubrication, enhanced oil recovery, corrosion, and microemulsion formation were discussed in detail. The results from this study showed that when an ionic surfactant is mixed with a nonionic surfactant in a one-to-one ratio, the molecular packing is enhanced [66]. Correspondingly, optimum properties such as corrosion resistance, enhanced oil recovery, melting point, evaporation retardation, foam formation, and surface viscosity were affected by the chain length compatibility. The rationale for the improvement in properties is that matching chain lengths allows for more stable interactions between surfactant molecules in the adsorbed layers [66,67].

12 Adsorption at Surface/Interface

12.1 Adsorption Basics

Surfactant adsorption is a prerequisite to surfactant-based surface coverage. A common interpretation of the adsorption of ionic surfactant on oppositely charged substrates is depicted in Fig. 1.7 with four adsorption regions (I, II, III, and IV) [68,69]. In this view the adsorption trends are linear in Region I due to electrostatic attraction. The adsorption density

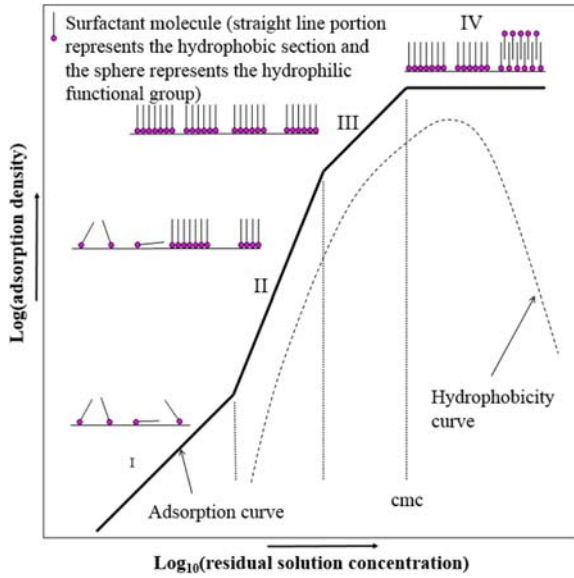

FIGURE 1.7 Qualitative comparison of adsorption density and residual ionic surfactant concentration on logarithmic scales with associated surfactant adsorption structures for an oppositely charged substrate.

follows the Gouy−Chapman equation with a constant slope under constant ionic strength conditions. The adsorption density of the ions (negative ions as an example), Λ_-, is given by the following equation [69]:

$$\Lambda_- = -\frac{\sigma_-}{zF} \tag{1.19}$$

where σ_- is surface charge density of solid surface/substrate and hardly changes under constant ionic strength conditions, F is the Faraday constant, and z is the valence charge of the ion.

Increased adsorption at higher surfactant concentration leads to Region II in which the adsorption density increases more than the corresponding solution concentration due to aggregate structure formation at the surface. The adsorbed surfactant can be in the form of hemimicelles due to lateral interactions between hydrocarbon chains that can lead to patches of packed molecules [69].

In Region III, electrostatic attraction is no longer operative due to the electrically neutralized solid surface by the adsorbed surfactant, and adsorption takes place due to lateral attraction alone with a reduced slope. Region IV is a saturated region with not much additional adsorption as the residual solution concentration increases because of solution micelle formation. The adsorption in this region is mainly through lateral hydrophobic interaction between the hydrocarbon chains. The local bilayer areas may be in the form of cylindrical or rod-like micelles, in which surfactant molecules adsorb with

a reversed orientation (head groups facing the bulk solution), resulting in a decrease in the hydrophobicity of the micelle in this region [68].

Nonionic surfactants usually contain polar head groups, which tend to form hydrogen bonds with the hydroxyl groups on the solid surface/substrate. The adsorption of nonionic surfactants to most solids is weaker than that of ionic surfactants considering that hydrogen bonding is weaker than electrostatic interaction. Therefore nonionic surfactants exhibit a sharp increase in Region III in the adsorption isotherm due to the absence of electrostatic interactions [66]. In other regions, nonionic surfactants and ionic surfactants exhibit similar characteristics in the adsorption isotherms [68].

Surface coverage on metals/metal oxides is directly determined by the effective adsorption of surfactant monolayers and bilayer/multilayers on the metal/metal oxides substrate/surface due to the physical and chemical blockage of the surface-active sites exposed to corrosive media [6,11,22,70]. Physisorption is usually accomplished through van der Waals forces and electrostatic interactions between polar or charged functional groups and a charged/polar surface [6,22,70]. The adsorbed surfactant chemically modifies some surfaces in a way that the functional groups partially donate electrons to the surface and link to the substrate by forming a partial chemical bond, leaving the hydrocarbon tails pointing outward and forming a densely packed hydrophobic barrier, which is believed to inhibit the diffusion of water, carbonate ions, halide ions, hydrogen ions, oxygen, and other species to the surface [70,71]. Adsorption behavior can usually be evaluated using experimental methods, such as Fourier-transform infrared (FTIR) spectroscopy and polarization modulation infrared reflection absorption spectroscopy [72,73], or using computational approaches such as density functional theory and classical molecular dynamics simulations [12,71,74–77]. More recently, the utilization of data mining-based artificial neural networks is becoming a trend in evaluation of surface adsorption on metals/metal oxides and corrosion inhibition [78,79], even though this method is purely empirical without physical meaning.

The adsorption of a surfactant molecule on a metal/metal oxide surface, which is an example of a solid/liquid interface, can be presented as a substitution adsorption process between the surfactant molecules in aqueous solution, (S_{aq}), and the water molecules on the surface (H_2O_{ad}) [80,81]:

$$S_{aq} + \varsigma\, H_2O_{ad} \leftrightarrow S_{ad} + \varsigma\, H_2O_{aq} \tag{1.i}$$

where ς is an empirical fitting parameter, which is interpreted as the number of water molecules displaced by one surfactant molecule.

12.2 Adsorption Isotherms

The most frequently used adsorption models are the Langmuir model, Temkin model, Freundlich model, Frumkin model, Flory–Huggins model,

Dhar–Flory–Huggins model, Bockris–Swinkels models, Bockris–Devanathan–Muller model, van der Waals–Stern model, and Stern Adsorption model [49,53,71,82–84], which are described.

The Langmuir adsorption isotherm assumes that all surface adsorption sites are equivalent, regardless of whether neighboring sites are occupied. Using the Langmuir model, the adsorbed adsorbate concentration is expressed as follows [71]:

$$\boldsymbol{K_{ad}C_m^w} = \frac{\boldsymbol{\theta}}{\boldsymbol{1-\theta}} \tag{1.20}$$

where θ is surface coverage, K_{ad} is the adsorption equilibrium constant, and C_m^w is the total concentration of monomeric surfactants in aqueous phase or available surface cites.

Determination of whether or not the Langmuir model applies to a given set of data can be made by plotting $1/\theta$ versus $1/C_m^w$ and evaluating the linearity of the data. The equilibrium adsorption constant, K_{ad}, can be calculated from the slope. K_{ad} can be used to calculate the free energy of adsorption as discussed previously. Some of the limitations of the Langmuir model are the neglect of molecular interactions, inability to account for multilayer coverage (along with all other general models), and the neglect of heterogeneous surface sites. However, despite its limitations, it is generally very effective and well used.

The associated equation for a multicomponent system expressed as a fraction of sites occupied (θ_i) is as follows [85]:

$$\boldsymbol{\theta_i} = \frac{\boldsymbol{K_{adi}C_{mi}^w}}{\boldsymbol{1+\sum_i K_{adi}C_{mi}^w}} \tag{1.21}$$

where $\boldsymbol{\theta_i}$ represents the surface coverage from surfactant i $\boldsymbol{K_{adi}}$ is equilibrium constant of surfactant i, and $\boldsymbol{C_{mi}^w}$ represents the monomeric concentration of surfactant i in aqueous solution.

The Temkin adsorption isotherm is an empirical adsorption model that considers nonuniform site distribution. According to this model, the adsorbed adsorbate concentration is expressed as:

$$\boldsymbol{K_{ad}C_m^w} = \boldsymbol{\exp(\xi\theta)} \tag{1.22}$$

where ξ is the molecular interaction constant ($\xi < 0$ indicates lateral attraction interactions between adsorbed surfactant molecules; and $\xi > 0$ indicates lateral repulsion interactions between adsorbed surfactant molecules). ξ takes into account of adsorbent–adsorbate interactions. This model usually assumes that heat of adsorption of all molecules in the layer decreases linearly rather than logarithmically with $\boldsymbol{\theta}$ when the extremely low and high values of concentrations are ignored [84].

The Freundlich adsorption isotherm is derived by assuming a site distribution function that is based on varying adsorption site free energy values. Using this model, the surface coverage can be expressed as follows:

$$K_{ad}C_m^w 1/\varsigma = \theta \tag{1.23}$$

where ς represents the number of water molecules displaced by one surfactant molecule as previously described. It reduces to the Langmuir equation for $\varsigma = 1$ at low concentrations and for $\varsigma = \infty$ at high concentrations. The value of $1/\varsigma$ is a measure of adsorption intensity or surface heterogeneity, indicating more heterogeneous surface as its value approaches 0. A value of $1/\varsigma$ below unity implies chemisorption whereas $1/\varsigma$ above one is an indication of cooperative adsorption [84].

The Frumkin isotherm can be represented by the following equation:

$$K_{ad}C_m^w = \frac{\theta}{(1-\theta)}\exp(-\xi\theta) \tag{1.24}$$

Similar to the Temkin isotherm, the Frumkin isotherm also considers lateral interactions between adsorbed surfactant molecules through ξ. Determination of whether or not the Frumkin model applies to a given set of data can be made by plotting $\ln\left(\theta/\left(C_m^w(1-\theta)\right)\right)$ versus θ and evaluating the linearity of the data.

The Flory–Huggins isotherm can express the feasibility and spontaneous nature of an adsorption process and takes the following format:

$$K_{ad}C_m^w = \frac{\theta}{\varsigma(1-\theta)^\varsigma} \tag{1.25}$$

The linear form of the Flory–Huggins model can be obtained by plotting $\ln\left(\theta/C_m^w\right)$ versus $\ln(1-\theta)$.

The Dhar–Flory–Huggins isotherm is similar to the Flory–Huggins model except for one exponential factor and has the following form:

$$K_{ad}C_m^w = \frac{\theta}{(1-\theta)^\varsigma \quad \exp(\varsigma-1)} \tag{1.26}$$

The linear form of the Dhar–Flory–Huggins model can be checked by plotting $\ln\left(\theta/C_m^w\right)$ versus $\ln(1-\theta)$. It has been shown that it is strictly incorrect to refer to an isotherm containing the configurational term $\theta/\varsigma(1-\theta)^\varsigma$ as the "Flory–Huggins isotherm," since Flory–Huggins statistics leads to an isotherm having a different form for the configurational term, which is $\exp(\varsigma-1)$.

The Bockris–Swinkels isotherm was originally proposed by Bockris and Swinkels for the evaluation of adsorption of organic compounds on metal electrode and takes the following form:

$$K_{ad}C_m^w = \frac{\theta}{(1-\theta)^\varsigma}\frac{(\theta+\varsigma(1-\theta))^{(\varsigma-1)}}{\varsigma^\varsigma} \tag{1.27}$$

Note that the Bockris–Swinkels isotherm reduces to the Langmuir isotherm when $\varsigma = 1$.

There are other isotherms available, such as the van der Waals–Stern model [30], the Stern Adsorption model [85], and the Hill–de Boer model [84], but they are not used as frequently as the above isotherms in the evaluation of surfactant adsorption on metal/metal oxide surface. Based on the experimental data, an appropriate adsorption isotherm can be selected for a particular surfactant of interest and the associated applications are provided elsewhere [6,71,86]. Note that all the isotherms are based on best fit of experimental data, and they are only partially theoretically sound except the Langmuir isotherm. The best-fit empirical parameters ς and ξ usually cannot be extrapolated to other surfactants that include homologous and nonhomologous surfactants.

Recently, a multiinteraction (MI) isotherm that describes monolayer adsorption and lateral interactions between adsorbed surfactant molecules and the formation of surface aggregates based on the combination of Langmuir isotherm and the aqueous cmc has been developed and described as follows [87]:

$$\boldsymbol{\Lambda_e} = \boldsymbol{\Lambda_{max,1}} \frac{\boldsymbol{C_m^w}/\boldsymbol{\Gamma^w}}{\boldsymbol{K_{haf,1}} + \boldsymbol{C_m^w}/\boldsymbol{\Gamma^w}} + \boldsymbol{\Lambda_{max,2}} \frac{\left(\boldsymbol{C_m^w}/\boldsymbol{\Gamma^w}\right)^{\varsigma}}{\boldsymbol{K_{haf,2}} + \left(\boldsymbol{C_m^w}/\boldsymbol{\Gamma^w}\right)^{\varsigma}} \tag{1.28}$$

where Λ_e is the equilibrium amount of adsorption concentration [10^7 molecules/colony-forming unit (CFU)]; $\Lambda_{max,1}$ and $\Lambda_{max,2}$ are the maximum adsorption concentrations for the two interactions; $K_{haf,1}$ and $K_{haf,2}$ are half saturation constants for each interaction (unit less); and Γ^w is the aqueous cmc. The first term on the right-hand side of the abovementioned equation is a Langmuir isotherm describing monolayer adsorption on the substrate surface, and the second term accounts for lateral interactions between the adsorbed surfactants and formation of the surface aggregates. The multiinteraction isotherm adsorption has been validated for linear polyoxyethylene (POE) alcohol surfactants with the form C_xE_y onto the surface of *Sphingomonas* sp. bacteria [87] and an example of the model application to $C_{12}E_9$ is given in Fig. 1.8. The fitting of an MI isotherm is excellent over the entire concentration above and below the aqueous cmc, while the Langmuir isotherm fails to fit well. However, note that the MI isotherm has three best-fit parameters (ς, $K_{haf,1}$, and $K_{haf,2}$) and that these parameters have the same limitation as those in the regular adsorption isotherms discussed previously. Correspondingly, the extrapolation of the fitting parameters to other surfactants usually leads to unreliable results.

The aqueous sac (represented using $\overline{\Gamma}$) and cmc (represented using Γ^w) are important parameters characterizing surfactant adsorption and aggregation. Therefore a new adsorption isotherm termed the modified Langmuir

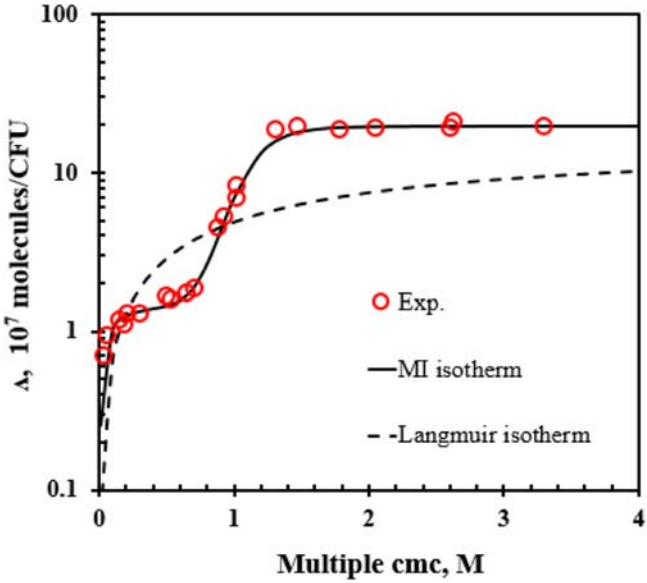

FIGURE 1.8 Comparison of experimental and fitted adsorption isotherms for $C_{12}E_9$ onto the *Sphingomonas* sp. *Replotted after Ref. [87].*

adsorption (MLA) has been reported by incorporating the aqueous cmc into the regular Langmuir model [6,11,13]. The concentration range is usually confined between zero and the cmc for accurate evaluation. The MLA is presented in the following:

$$\frac{1}{1-\theta} = 1 + K' \frac{C_m^w}{\Gamma^w} \tag{1.29}$$

where K' is equal to the adsorption constant K_{ad} multiplied by Γ^w. The value of K' for homologous surfactants is relatively constant and can be used as a universal constant for such homologous surfactants. Note that the monomeric concentration in aqueous phase C_m^w can increase up to the aqueous cmc Γ^w or above. The sac/cmc is a transition point in characterizing the effectiveness of adsorbed surfactants in formulating a surface coverage film. On the other hand, the surface coverage is usually high enough at the sac, and therefore the continuous increase of surfactant concentration up to the sac/cmc or above does not contribute much to additional surface coverage. Thus, the deviation between MLA prediction and experimental results at or above the sac/cmc should be small.

The essence of MLA is that the incorporation of cmc can successfully adjust for the effects of solution conditions and surfactant properties, such as

salt concentration, solution temperature, hydrocarbon chain length, lateral surfactant interactions, and counterion binding, on surfactant adsorption and thus on corrosion inhibition efficiency. It is interesting to note that the regression parameter K' in MLA for one surfactant can be transferred (extrapolated) to the corresponding homologous surfactants and other surfactants with similar head groups (usually characterized by quantum descriptors) [6,11,13].

The plots of MLA and some commonly used adsorption models based on the electrochemical measurements for a surfactant mixture ($C_{12}/C_{14}/C_{16} = 0.70/0.25/0.05$ in 0.171 M NaCl aqueous media with CO_2 saturation and pH = 4 at 40°C) are presented in Fig. 1.9 in which only MLA shows clearly the feature of the aqueous sac [6,11]. The MLA plot of $\left(1/(1-\theta)\right)$ versus C_m^w/Γ^w yields a slope of fit parameter $K' = 13.74$, and an intercept of 1 which is in the absence of surfactant inhibitors, as shown in Fig. 1.9D. The $K' = 13.74$ can be extrapolated to other mixtures of BAC surfactants to predict surface coverage, which is comparable to experimental data as shown in Fig. 1.10 [6,11].

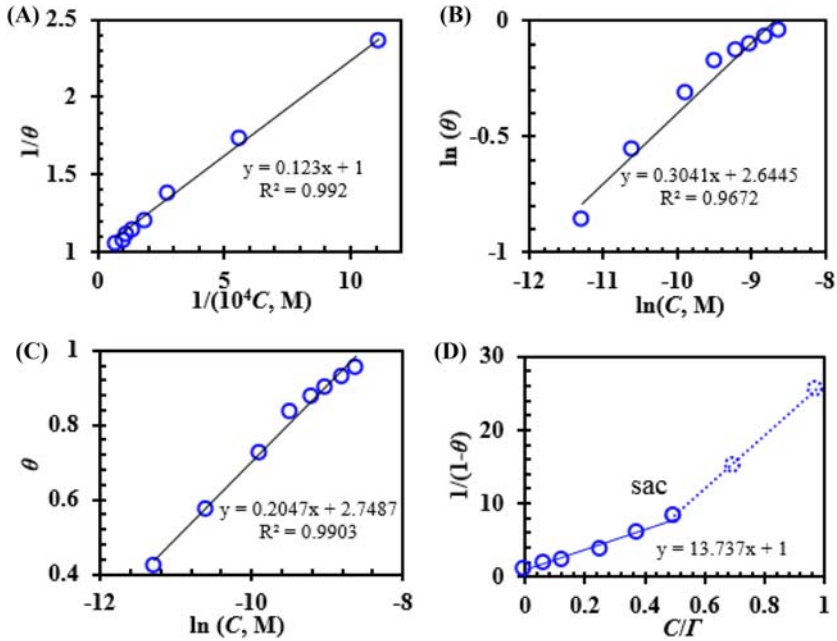

FIGURE 1.9 The adsorption isotherms on X65 steel electrode of mixed BAC ($C_{12}/C_{14}/C_{16} = 0.70/0.25/0.05$) in 0.171 M NaCl aqueous media with CO_2 saturation and pH = 4 at 40°C: (A) Langmuir adsorption, (B) Freundlich adsorption, (C) Temkin adsorption, and (D) MLA. *BAC*, Benzalkonium chlorides; *MLA*, modified Langmuir adsorption.

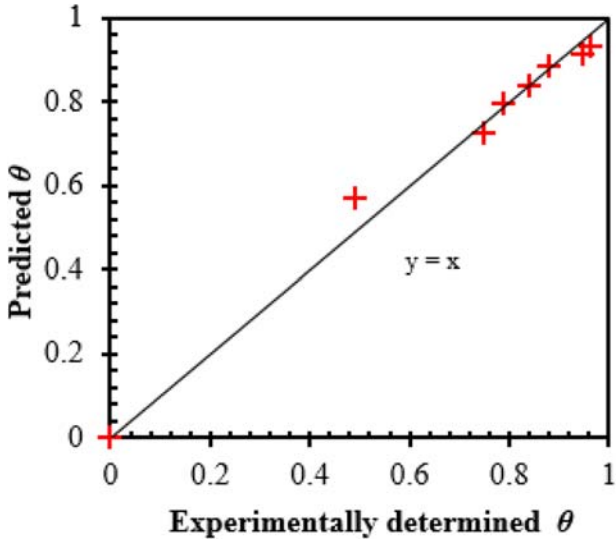

FIGURE 1.10 The comparison of experimentally determined surface coverage and predicted surface coverage based on MLA and extrapolated parameter $K' = 13.74$ on X65 steel electrode of mixed BAC ($C_{12}/C_{14}/C_{16} = 1/1/1$) in 0.599 M NaCl aqueous media with CO_2 saturation and pH 5 at 40°C. *BAC*, Benzalkonium chlorides; *MLA*, modified Langmuir adsorption.

12.3 Adsorption Thermodynamics

The standard free energy of surfactant adsorption for the adsorption−solution equilibrium is given by the following equation [11]:

$$\Delta G^{o}_{ad} = -RT\ln\frac{a_{S_{ad}}}{a_{S_{aq}}} = -RT\ln\frac{C_{S_{ad}}}{C_{S_{aq}}} \tag{1.30}$$

where a is the activity and C represents the concentration of the specified form of the surfactant either adsorbed or in aqueous phase. Note the activity coefficient for the aqueous and adsorbed forms is assumed to be equivalent, thereby canceling its effect in the equation. Thus the equation can be rearranged to:

$$C_{S_{aq}}\exp\left(-\frac{\Delta G^{o}_{ad}}{RT}\right) = C_{S_{ad}} \tag{1.31}$$

The concentration of adsorbed surfactant is effectively the surface excess concentration per unit area, Λ, divided by the thickness of the adsorbed surfactant layer, which is the same scale as the length of the surfactant molecule, l_m. The concentration of surfactant in the aqueous phase is effectively

the bulk concentration of surfactant. Therefore the surface excess concentration per unit area for equilibrium adsorption can be rewritten as [88]:

$$\Lambda = C_{S_{aq}} l_m \exp\left(-\frac{\Delta G^o_{ad}}{RT}\right) \tag{1.32}$$

Correspondingly, the surface excess at various surfactant concentration levels can be determined. Furthermore, the change in free energy associated with adsorption can be calculated using the rearranged form of the following equation:

$$\Delta G^o_{ad} = -RT\ln\left(C_{S_{aq}} l_m\right) + RT\ln\Lambda \tag{1.33}$$

Alternatively, the free energy of adsorption can be determined from the equilibrium adsorption constant [11]:

$$\Delta G^o_{ad} = -RT\ln(C_{mw} K_{ad}) \tag{1.34}$$

Here C_{mw} is the molar concentration of water.

Thus, the free energy of adsorption can be determined from equilibrium adsorption data. Temperature has a strong influence on surfactant adsorption. The relationship between free energy and temperature can be written in a traditional thermodynamic format:

$$\Delta G^o_{ad} = \Delta H^o_{ad} - T\Delta S^o_{ad} \tag{1.35}$$

Because surfactant adsorption is commonly an exothermic process, the enthalpy term in this equation is usually negative. To have the required negative change in free energy for the reaction, the entropy term must be smaller than the enthalpy term because the entropy for adsorption of surfactant is negative due to the ordering of the system associated with adsorption of surfactant. Thus, if temperature increases, the entropy term, which has an overall positive sign, eventually becomes more dominant than the negative enthalpy term, and desorption occurs. This same effect is manifest in adsorption kinetics. Temperature also increases the rate of adsorption, but the corresponding increase in the desorption process becomes more dominant in relation to the net equilibrium. Consequently, increasing the temperature generally decreases the adsorption efficiency of surfactant molecules.

The enthalpy of adsorption is related to the change in equilibrium adsorption constant with respect to the change in temperature [85]:

$$\left(\frac{\partial \ln K_{ad}}{\partial T}\right)_\theta = \frac{\Delta H^o_{ad}}{RT^2} \tag{1.36}$$

Differentiation for constant coverage and comparison to enthalpy change leads to [85]:

$$\left(\frac{\partial \ln C_{S_{aq}}}{\partial T}\right)_{\theta} = -\left(\frac{\partial \ln K_{ad}}{\partial T}\right)_{\theta} = -\frac{\Delta H^{o}_{ad}}{RT^{2}} \tag{1.37}$$

The change in the concentration or molality of adsorbate as a function of temperature at constant coverage is proportional to the enthalpy change [85]:

$$\left(\frac{\partial \ln C_{S_{aq}}}{\partial (1/T)}\right)_{\theta} = \frac{\Delta H^{o}_{ad}}{R} \tag{1.38}$$

Consequently, a plot of the logarithm of bulk surfactant concentration versus the change in inverse temperature has a slope equal to the enthalpy change associated with adsorption divided by R.

The entropy of adsorption is influenced by the ordering that occurs when molecules adsorb in an ordered structure on a surface. However, the adsorption of surfactant on a surface is accompanied by desorption of water molecules and adsorbed ions that become disordered as they leave the surface. One approach to determine the enthalpy and the entropy of adsorption is to perform adsorption tests at different temperatures then plot the free energy of adsorption versus temperature. Because free energy is related to enthalpy and entropy, a plot of adsorption free energy versus absolute temperature provides a slope equal to the entropy of adsorption and an intercept equal to the enthalpy.

12.4 Adsorption Kinetics

Surfactant adsorption is affected by the packing efficiency of surfactant molecules and their competition with other species (water molecules, halides, organic acids, and other species). Reports are available from mechanistic modeling and molecular modeling perspectives regarding the packing efficiency; however, studies assessing the kinetic aspect of surfactant adsorption are very limited [71]. Therefore the comprehensive evaluation of the transport of water, halides, carbonate ions, hydrogen, and metal complexes through the porous adsorbed surfactants from the kinetic perspective is expected. On the other hand, the surfactant concentration in aqueous solution decreases as a function of time due to desorption. Understanding adsorption and desorption kinetics of surfactants is critical in the optimization of injection frequency of surfactants to ensure effective surfactant adsorption and surface coverage [24,89–91].

The extent and rate of adsorption of many surfactants are affected by surfactant concentration as well as concentration of competitive ions. As an example, the rate of sodium oleate adsorption on a fluorite surface is reduced significantly by the presence of competitively adsorbing ions such as

hydroxide, carbonate, and fluoride ions. Measurements made using FTIR internal reflection spectroscopy, a continuous flow cell, and a fluorite internal reflection element showed that anions strongly influence the rate of oleate adsorption on fluorite [37,92]. Hydroxide has the most pronounced influence on adsorption kinetics significant in the 0.0001 M concentration regime, followed by carbonate and then fluoride [37,92].

Adsorbed surfactant molecules become more oriented as they pack more tightly. In a comparison of LB monolayers and self-assembled (SA) monolayers of stearate, Jang and Miller [93] found that stearate molecules were oriented 9−16 degrees from the surface normal for LB monolayers and 21 degrees for SA monolayers. Spectroscopic information was also used to determine the stearate molecules predominantly in the transition state.

For a first-order reaction described by Eq. (1.i), it can be shown that [37,94]:

$$\frac{d\theta}{dt} = k_f C_{S_{aq}}(1-\theta) \tag{1.39}$$

where represents the surface coverage, k_f represents the forward reaction rate constant, t represents reaction time, and $C_{S_{aq}}$ represents the bulk concentration of adsorbing species. Integration of Eq. (1.39) leads to [37,94]:

$$\ln\left(\frac{1}{1-\theta}\right) = k_f C_{S_{aq}} t \tag{1.40}$$

assuming no coverage at time zero. Thus, for constant solution concentration, plotting $\ln\left(1/(1-\theta)\right)$ versus t, should yield a slope of $k_f C_{S_{aq}}$ and a zero intercept if the kinetics follow Eq. (1.40) assuming a first-order reaction with respect to the adsorption density at constant bulk concentration. Fig. 1.11 illustrates such a plot for the adsorption of 1×10^{-5} M oleate on fluorite in which the maximum monolayer-level adsorption density was selected between the realistic monolayer coverage values of 5.8 and 6.8 mol/m^2 based upon LB film results [37], such that the best fit of the data was obtained as determined by maximizing the R-squared values. As predicted by Eq. (1.40), a reasonably linear relationship exists between $\ln\left(1/(1-\theta)\right)$ and time as illustrated in Fig. 1.11. The linear relationship is accompanied by an intercept near zero, though it should be noted that for the regression analysis the line was forced through zero. The first-order kinetics seems to be suitable at a concentration of 1×10^{-5} M oleate.

Chen and Frank have shown that adsorption kinetics follow a modified Langmuir−based kinetic model that is expressed as [95]:

$$\frac{d\theta}{dt} = \frac{k_f}{C_o} C_{S_{aq}}(1-\theta) - \frac{k_b}{C_o}\theta \tag{1.41}$$

where k_f represents adsorption rate constant, k_b represents desorption rate constant, and C_o is the concentration of adsorbed surfactant at full coverage.

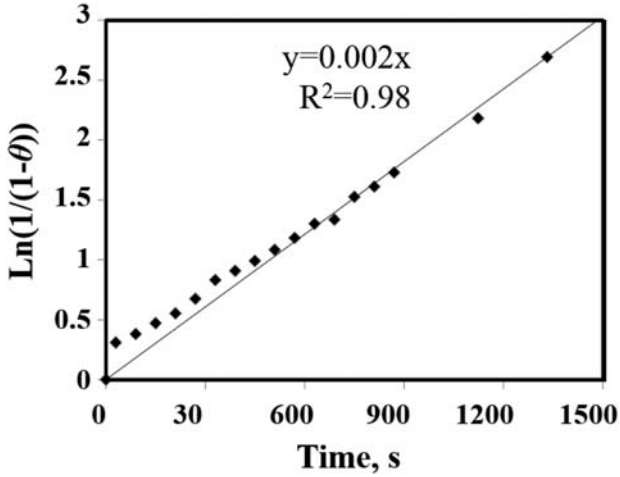

FIGURE 1.11 Plot of $\ln\left(1/(1-\theta)\right)$ versus time for linoleate adsorption at a fluorite surface as measured from in situ FTIR/IRS at 25°C. The linoleate concentration was 1×10^{-5} M. The maximum adsorption density was set at 6.2 μmol/m^2. *FTIR/IRS*, Fourier-transform infrared internal reflection spectroscopy.

A kinetic model for adsorption at an expanding air−water interface has been developed by Valkovska and coworkers [30] This model incorporates Fick's second law of diffusion with traditional adsorption isotherm modeling to predict adsorption at an expanding air−water interface. Valkovska and coworkers tested this model with alkyltrimethylammonium bromide surfactants in 0.1-m sodium bromide solution and found reasonable agreement between the model and the measured data. This model is very complex and does not seem to fit the data any better than simpler models. However, it does consider micelle breakdown, and it may be useful for some applications with rapidly changing interfacial areas.

13 Surfactant Aggregation and the Aqueous cmc

As mentioned previously, the incorporation of the aqueous cmc into MLA provides a substantial improvement in the modeling of surfactant adsorption in that this method can describe surfactant adsorption on substrate surface and account for lateral interactions among the adsorbed surfactants, formation of aggregates, and the environmental factors such as salt concentration and solution temperature. Therefore, the accurate evaluation of the aqueous cmc of pure and mixed surfactants of interest is critical to the application of MLA. On the other hand, the aggregation process consumes most of the surfactants added to the aqueous phase above the aqueous cmc, which inevitably affects the availability of monomeric surfactants for adsorption on metal surface [71,89].

Assuming the monomeric (ionic) surfactant m_i ($i = 1$, 2, or 3…) is completely dissociated in aqueous solution containing counterion m_j ($j = 1$, 2, or 3…) but in the micelle form the surfactant is associated to some extent with counterions, the surfactant micellization can be described by the following process [96,97]:

$$N\sum_i \alpha_i \mathbf{m}_i^{z_i} + N\sum_j \delta_j \mathbf{m}_j^{z_j} \leftrightarrow \mathbf{M}_N^{N\left(\sum_i \alpha_i z_i + \sum_j \delta_j z_j\right)} \tag{1.42}$$

where α_i is the molar fraction of surfactant i in the micelle, M_N, which has an aggregation number N, micelle composition α_i, and an ion binding coefficient δ_j. For micelles of pure surfactant, $\alpha_i = 1$; for mixed micelles, $0 < \alpha_i < 1$. z_i and z_j are the valences of ionic surfactant i in dissociated form and ion j. For nonionic surfactant i, $z_i = 0$ and $\delta_j = 0$.

One of the challenges in the study of the aqueous cmc comes from the effects of specific ions and added salts on the aggregation properties of surfactants. Different counterions usually have different effects on the aqueous cmc, micelle shape, micelle size and distribution, mixed micelle composition (for mixed surfactants), and phase separation [71,98–100]. It is reported that the counterion effect on the aggregation properties of cationic surfactants is usually stronger than that of anionic surfactants [101]. In addition, the cmc depression due to the counterion effect usually follows the Hofmeister series: $OH^- < F^- < Cl^- < Br^- < NO_3^- < ClO_3^- < I^- <$ benzoate$^-$ < salicylate$^-$ for cationic surfactants and $Li^+ < Na^+ < K^+ < Cs^+$ for anionic surfactants [56,97]. The specific counterion effects on micelle size and sphere-to-rod transition are usually in the same order as shown for cmc. The counterion binding mechanism, however, is not clear and has been a controversial issue [102]. At low salt concentration, the coion effect on cmc, aggregation number, and sphere-to-rod transition is negligible [103,104]. However, as salt concentration increases, the coion effect becomes increasingly noticeable.

It is reported that an alternative molecular thermodynamic (AMT) model [89,96] for the prediction of the aqueous cmc has been developed, which incorporates the surfactant activity, counterion activity, and ion effects on surfactant aggregation. The aqueous cmc of pure surfactant i (Γ_i^w), or of surfactant mixture (Γ^w), is calculated using the equation below (Γ^w is used for illustration) [96,97]:

$$\boldsymbol{\Gamma^w} = (\boldsymbol{C_{mw}} + \boldsymbol{C_s})\mathbf{exp}^{\left(\frac{1}{kT}\Delta\mu_m^o\right)} \tag{1.43}$$

where C_{mw} is molar concentration of water, C_s is concentration of salt, k is the Boltzmann constant, T is temperature, and $\Delta\mu_m^o$ is micellization free energy that is calculated from several contributing thermodynamic terms [96]:

$$\Delta\boldsymbol{\mu}_{\mathbf{m}}^{\mathbf{o}} = \Delta\boldsymbol{\mu}_{\mathbf{trt}}^{\mathbf{o}} + \Delta\boldsymbol{\mu}_{\mathbf{int}}^{\mathbf{o}} + \Delta\boldsymbol{\mu}_{\mathbf{pack}}^{\mathbf{o}} + \Delta\boldsymbol{\mu}_{\mathbf{st}}^{\mathbf{o}} + \Delta\boldsymbol{\mu}_{\mathbf{ent}}^{\mathbf{o}} + \Delta\boldsymbol{\mu}_{\mathbf{elec}}^{\mathbf{o}} + \Delta\boldsymbol{\mu}_{\mathbf{act}}^{\mathbf{o}} \tag{1.44}$$

The first three terms on the right side of Eq. (1.44) are associated with the packing and interactions of hydrocarbon tails and the formation of a

hydrophobic micellar core: $\Delta\mu^{o}_{trt}$, $\Delta\mu^{o}_{int}$, and $\Delta\mu^{o}_{pack}$ represent free energy contributions from hydrocarbon transfer from water into micelle, formation of micellar core−water interface, and hydrocarbon tail packing in micelle, respectively. The next three terms are associated with surfactant head groups and counterions in the micelle−water interfacial region: $\Delta\mu^{o}_{st}$, $\Delta\mu^{o}_{ent}$, and $\Delta\mu^{o}_{elec}$ represent surfactant head group steric interactions, head group−counterion mixing, and electrostatic interactions, respectively. The last term $\Delta\mu^{o}_{act}$ represents the contribution from surfactant activity and counterion activity in the bulk solution.

Application of the model in Eq. (1.44) to pure alkyltrimethylammonium surfactant C_nTABr in solution with added salt (NaBr, NaCl, or KCl) to evaluate chain length effects, counterion effects, and coion effects on aggregation properties is shown in Fig. 1.12 [13,89,96,97]. The aqueous cmc (Fig. 1.12A) and the sphere-to-rod transition threshold

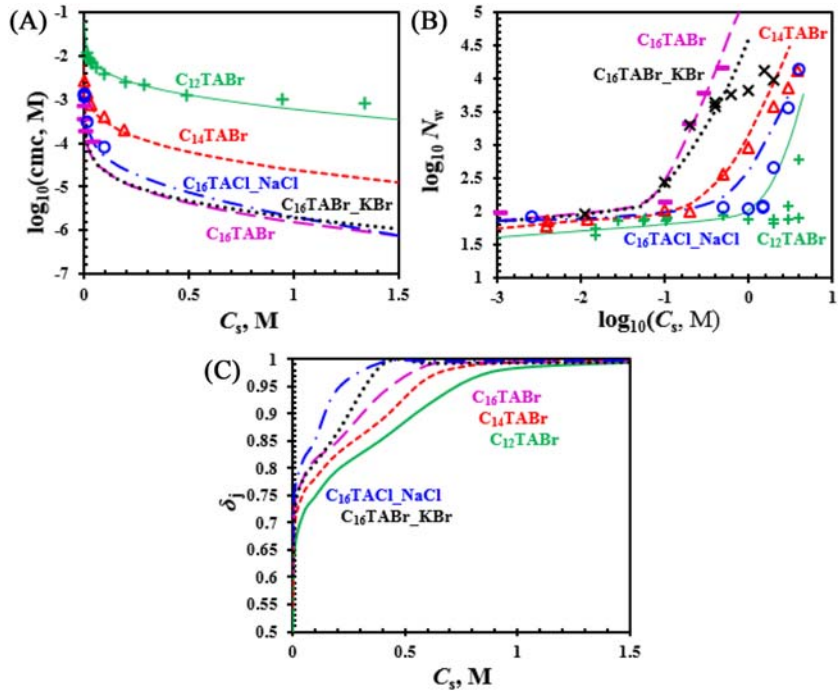

FIGURE 1.12 Comparison of predicted parameters and experimental parameters of aggregation: (A) cmc, (B) weight-based aggregation number N_w, and (C) counterion binding coefficient of C_nTAX (X = Br^-, Cl^-) vs salt concentration. The salt type is specified in the plots; otherwise, the salt is defaulted to NaBr. Solid and dashed lines represent model prediction; symbols represent experimental data from Ref. [71]. Model inputs are based on experimental conditions: total concentration of surfactant set at 10 mM for C_{14}TABr and C_{16}TABr/Cl, and at 30 mM for C_{12}TABr at temperature of 35°C. *cmc*, Critical micelle concentration.

(Fig. 1.12B) decreases as chain length increases whereas the weight-based aggregation number N_w (Fig. 1.12B) increases as chain length increases. The predicted aqueous cmc for all surfactants in Fig. 1.12 matches very well with experimental data, except that a slight deviation appears for C_{12}TABr with added NaBr above 1 M. Excellent agreement is observed between predicted and experimental N_w values. The sphere-to-rod transition is manifested by the sharp change of aggregation number, counterion binding coefficient, and core minor radius (not shown here) as a function of salt concentration. The comparison of model predicted transition (salt concentration threshold) and deduced transition from experiment match reasonably well [38,97,105–109]. For C_{16}TABr with added salt KBr, for example, the predicted threshold is 0.08 M and the experimental threshold is 0.1 M [38,110].

It is reported that the AMT model can also be applied to ternary surfactant mixtures, such as cationic/cationic/nonionic mixture: C_{16}TABr/C_{16}BzCl/$C_{16}E_{20}$ with added NaCl in the aqueous solution, as shown in Fig. 1.13 [89,96,97]. The comparison to the Clint model [111] and to the Rubingh and Holland (R-H) model [112] was also included. The predicted aggregation number is calculated only from the AMT model, which gives slightly overestimated but reasonable values.

An improved traditional model [6,11] for the prediction of the aqueous cmc is also reported and given below for various pure, binary, ternary, and multiple homologous/nonhomologous surfactant mixtures:

$$\boldsymbol{\Gamma}^{\mathbf{w}} = \frac{\boldsymbol{1}}{\sum_i \boldsymbol{x_i}\left(\boldsymbol{\gamma_c C_c}\right)^{\boldsymbol{\delta_i}}\left(1/\boldsymbol{\Gamma_i^p}\right)^{(\mathbf{1}+\boldsymbol{\delta_i})}} \tag{1.45}$$

where x_i is the bulk mixed molar fraction of surfactant i. Γ_i^p is the aqueous cmc of surfactant i in pure water (i represents surfactant 1, 2, or 3, ...). δ_i is counterion binding coefficient with respect to surfactant i based on best fit of experimental data. δ_i is nearly constant for a series of homologous surfactants and is also constant as a function of salt concentration (low to medium depending on specific surfactant class: 0–1). Note that the counterion binding coefficient δ_j in the advanced cmc model is with respect to counterion j and different from δ_i. C_c is the concentration of ions dissociated from electrolyte and from ionic surfactant in aqueous solution. γ_c is the mean activity coefficient of ions in aqueous solution and is usually calculated using Pitzer's method [113] or the Davies equation [114]. Eq. (1.45) is supported by the report that the cmc is heavily dependent on and exponentially related to electrolyte concentration [115,116].

It is clear that the aqueous cmc prediction model, for example, MLA, takes into account the ion/salt effect on aggregation/adsorption, head group–counterion pair and associated hydration effect, hydrocarbon chain length, steric interactions between head groups, electrostatic interactions at the

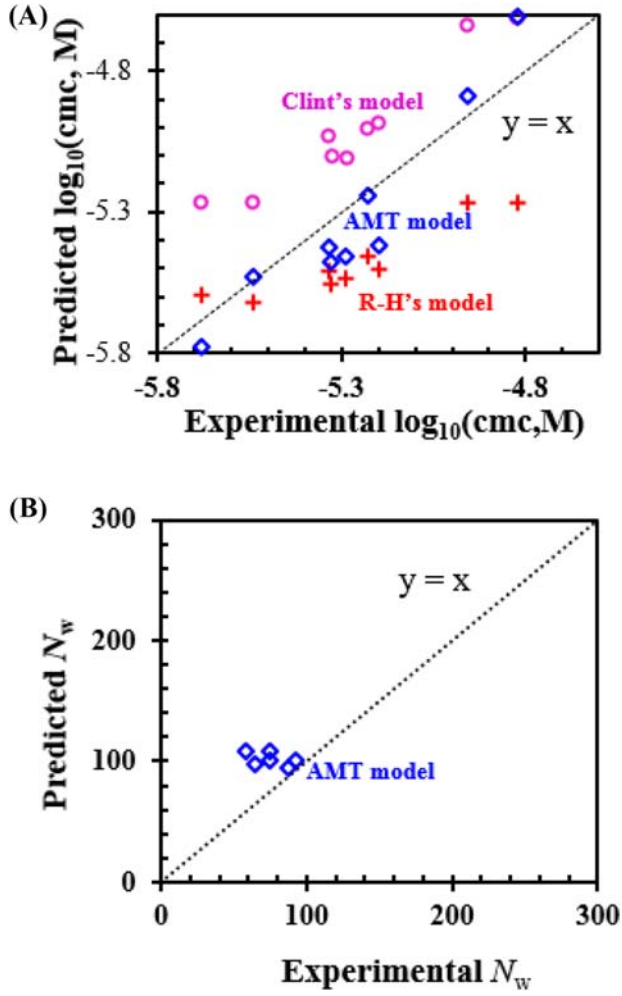

FIGURE 1.13 Predicted (A) cmc, and (B) aggregation number of ternary mixed surfactants alkyltrimethylammonium bromide C_{16}TABr, benzyldimethylhexadecylammonium chloride C_{16}BzCl, and polyoxyethylene (20) cetyl ether $C_{16}E_{20}$ versus experimental results. Predicted values in part (B) were calculated using AMT model. Inputs of model according to experiment conditions: total surfactant concentration set at cmc in 30-mM NaCl solution at 25°C. *AMT*, Alternative molecular thermodynamic; *cmc*, critical micelle concentration.

interfacial region of micelles, and the interactions between solvent and surfactant. Therefore, the insertion of the aqueous cmc into the Langmuir isotherm, which is the MLA as introduced previously, can accurately describe the adsorption of surfactants on substrates and associated effects of physical and chemical properties of surfactants and solvent environments.

14 Surfactant Partitioning Between Water and Oil

Surfactant molecules form different phases in water and oil and their mixtures. A general phase diagram is shown in Fig. 1.14 [117]. This figure shows that there are often several types of surfactant-mediated structures that form in water−oil−surfactant mixtures.

In a solution containing oil and water, surfactant molecules can be found to be in equilibrium in several forms under certain conditions. Surfactant can partition to the oil and aqueous phases; it can adsorb on solid surfaces; it can form dimers and micelles; it can combine with metals or hydrogen ions to form metal salts and hydrogenated compounds; and it can form other compounds. It is anticipated that solving all of the equilibrium processes simultaneously can be used to determine the surfactant concentration for effective adsorption, which can then be used in combination with methods for surface adsorption to predict the associated surface coverage by surfactants on metal/metal oxide surface.

When an aqueous surfactant solution comes into contact with an immiscible organic liquid, such as oil, surfactant monomers may prefer partitioning into organic liquid until equilibrium is reached between the two liquids

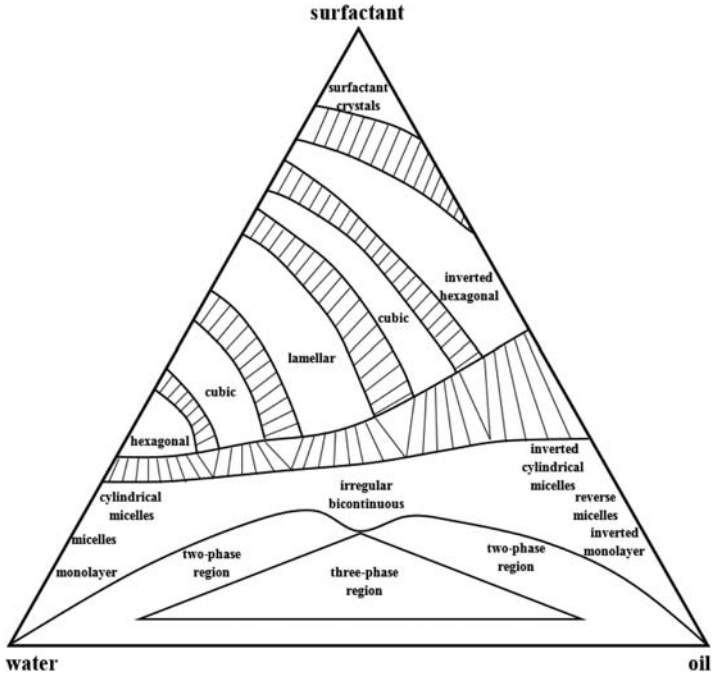

FIGURE 1.14 Phase diagram for surfactant, water, and oil illustrating different phase regions for a typical alkane oil and alkyl surfactant.

[118,119]. Considering the complexity of water/oil partitioning of surfactants in water−oil environment and associated interfacial phenomena, the determination of surfactant partitioning between water and oil usually serves as the basis of the hydrophobic−hydrophilic balance, which further affects the availability of monomeric surfactants in aqueous phase and the associated adsorption on metal/metal oxides surfaces.

For pure surfactant the partitioning is usually characterized by the partitioning coefficient, which is defined as the ratio of monomeric surfactant concentration in oil to that in aqueous phase (pure water or salt-containing water) [14,120]:

$$K_i = \frac{C_{\mathrm{mi}}^{\mathrm{o}}}{C_{\mathrm{mi}}^{\mathrm{w}}} \tag{1.46}$$

where K_i is the partitioning coefficient of surfactant i, $C_{\mathrm{mi}}^{\mathrm{o}}$ and $C_{\mathrm{mi}}^{\mathrm{w}}$ are monomeric concentration of surfactant i in oil phase and aqueous phase, respectively.

Extensive research has been performed on low concentration (typically lower than the aqueous cmc) partitioning of nonionic surfactants [119−130]. The partitioning research on higher surfactant concentration systems, however, is limited and has been rarely reported [121,131−133]. However, the investigation of partitioning above the aqueous cmc and the apparent cmc is important (the apparent cmc is the average concentration in water and oil environment at which the micelle starts to form): the partitioning is a monomer process, and the partitioning coefficient is determined by monomer concentrations in the two phases, which are limited by micelle formation.

For surfactant mixtures the partitioning becomes more complicated in terms of equilibrium mixture composition in each phase, because of the effect of individual mixed species on the partitioning, and the adsorption of mixture at the oil/water interface. It has been shown that for some pure surfactants, a plateau concentration of monomer is reached either in the oil phase or in the aqueous phase with increasing total surfactant concentration beyond the aqueous cmc [121,133]. However, the amounts of surfactants partitioned into the oil phase continue to increase beyond the aqueous cmc. The partitioning change of mixed surfactants above the aqueous cmc is reported to arise from the selective partitioning of more hydrophobic components into oil phase, which makes the experimental investigation and quantitative modeling work more challenging.

Before moving on to the discussion of partitioning modeling, it is necessary to clarify the relation between partitioning and the aqueous cmc. The aqueous cmc of pure surfactant or mixed surfactants in the absence of oil phase is assumed to be equal to the aqueous cmc in the presence of nonpolar oil phase, which is confirmed by related reports [14,70]. On the other hand, the nonpolar oil phase does not contribute to the micelle formation in aqueous phase. It is actually reported that for nonionic surfactants with nonpolar

heptane as oil phase, the aqueous cmc has been observed to be very similar to the corresponding aqueous cmc without the oil phase [134] and that for certain anionic surfactants with heptane as the oil phase, the aqueous cmc has also been found to be very close to the cmc measured in water in the absence of oil [135]. For certain cationic surfactants with a more polar oil phase (dichloromethane), however, the aqueous cmc in the absence of the oil phase is significantly different from the corresponding cmc in the presence of the oil phase [136].

It has been reported that the partition coefficients of surfactant in pure water/oil environment can be predicted using semiempirical modeling [122,129] and quantum chemical methods [137,138]. One quantum prediction of partitioning coefficient has been reported to take into account the effect of protonation in aqueous phase [24], which is, however, far away from realistic conditions in oilfields where the aqueous phase contains multiple classes of inorganic salts, and the crude oils are complex mixtures of organic solvents.

An improved surfactant partitioning prediction model termed Water−Oil−Surfactant Distribution Model (WOSDM) has been reported for the evaluation of partitioning and distribution of mixed surfactants in water (containing salts) and oil environment [14]. With this model the partitioning coefficient K_i of surfactant i is predicted using the following equation:

$$K_i = \frac{\gamma_{\mathrm{mi}}^{\mathrm{w}} C_{\mathrm{mo}}}{\gamma_{\mathrm{mi}}^{\mathrm{o}} C_{\mathrm{mw}}} \exp\left(- \frac{\Delta \mu_{\mathrm{tri}}^{\mathrm{o}}}{RT} \right) \tag{1.47}$$

where $\gamma_{\mathrm{mi}}^{\mathrm{o}}$ and $\gamma_{\mathrm{mi}}^{\mathrm{w}}$ are activity coefficients of monomeric surfactant i in oil phase and water phase, respectively. $\gamma_{\mathrm{mi}}^{\mathrm{o}}$ is usually assumed to be unity. For ionic surfactant, $\gamma_{\mathrm{mi}}^{\mathrm{w}}$ is equal to the geometric mean of the activity coefficient of counterion and the activity coefficient of hydrocarbon tail, whereas for nonionic surfactant, $\gamma_{\mathrm{mi}}^{\mathrm{w}}$ is equal to the activity coefficient of hydrocarbon tail. The activity coefficient of ions/counterions is evaluated using Pitzer's method [113] or the Davies equation [114] depending on the salt concentration, whereas the activity coefficient of the hydrocarbon tail is evaluated from the Setchenov equation [139]. The essence of $\gamma_{\mathrm{mi}}^{\mathrm{w}}$ is to take into account the effect of dissolved salt in water on water−oil partitioning of surfactants. C_{mo} and C_{mw} are molar concentrations of oil and water, respectively. The standard free energy change of transfer of surfactant i, $\Delta\mu_{\mathrm{tri}}^{\mathrm{o}}$, from water to oil is estimated from two methods. Method I is the free energy transfer method [14], in which $\Delta\mu_{\mathrm{tri}}^{\mathrm{o}}$ is calculated as the sum of the head group transfer energy and the hydrocarbon tail transfer energy. Method II is the quantum chemical method [24], in which $\Delta\mu_{\mathrm{tri}}^{\mathrm{o}}$ is interpreted as the difference in solvation energy of surfactant i in oil and in water based on the quantum chemical calculations using simulation software, such as Gasussian09. Excellent agreement is observed between predicted and experimental values of K_i for various surfactants as shown in Fig. 1.15.

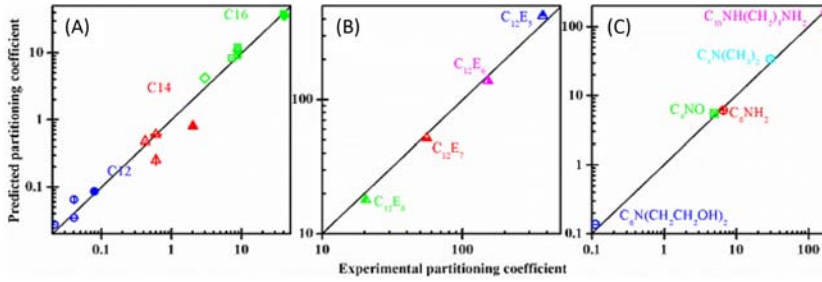

FIGURE 1.15 Comparison of the predicted partitioning coefficients and the experimental partitioning coefficients: (A) the partitioning coefficients of pure BAC surfactants C_{12}, C_{14}, and C_{16} between water and oil (toluene) at 40°C. [*For symbols in (A), open symbols with vertical center-cross line: transfer free energy calculated using Method II; all other symbols: transfer free energy calculated using Method I. Open symbols: 0 M in NaCl water; open symbols with center dot: 0.0342 M NaCl in water; open symbols with (vertical and horizontal) center-cross line: 0.171 M NaCl in water; half-filled symbol: 0.804 M NaCl in water; solid-filled symbols: 0.856 M NaCl in water.*] (B) The partitioning coefficients of polyoxyethylene alkyl ether ($C_{12}E_n$) in pure water and isooctane environment at 25°C. (C) The partitioning coefficients of N-based alkyl amines and derivatives in 0.1 M NaOH water and heptane at 20°C. *BAC*, Benzalkonium chlorides.

Assuming the amount of adsorbed surfactants in the oil−water interface is negligible, a mass balance of total mixed surfactants in the water−oil environment is given by the following equation [14]:

$$\boldsymbol{C_{tol}V_w = \overline{C} \quad (V_w + V_o)} \tag{1.48}$$

where C_{tol} is the initial concentration (not at equilibrium) of total surfactants added to aqueous phase; $\overline{C}$ is the overall average concentration of total surfactants in water−oil environments; V_o and V_w are volumes of oil and water, respectively.

When $\overline{C} < \Gamma^{ap}$ (Γ^{ap} is the apparent cmc, which is defined as the average concentration of mixed surfactants at which mixed micelles start to form in water−oil environments), mass balance of each mixed surfactant i at partitioning equilibrium is given by the following equation [14]:

$$\boldsymbol{x_i C_{tol} V_w = C^w_{mi} V_w + C^o_{mi} V_o} \tag{1.49}$$

The partitioning coefficient of surfactant mixture is termed the apparent partitioning coefficient and is given by the following equation:

$$\boldsymbol{K_{mix} = \frac{C^o_m}{C^w_m} = \frac{\sum C^o_{mi}}{\sum C^w_{mi}}} \tag{1.50}$$

where C^o_m and C^w_m are total concentrations of monomeric surfactants in oil and aqueous phases, respectively.

Substitution of Eqs. (1.48) and (1.49) into Eq. (1.50) leads to [14]:

$$K_{\mathrm{mix}} = \frac{\sum K_i x_i/(V_{\mathrm{w}} + V_{\mathrm{o}} K_i)}{\sum x_i/(V_{\mathrm{w}} + V_{\mathrm{o}} K_i)} \tag{1.51}$$

where x_i is the molar fraction of surfactant i in total mixed surfactants in bulk solution. Eqs. (1.49) and (1.51) are only applicable to the condition of $\overline{C} < \Gamma^{\mathrm{ap}}$, whereas Eqs. (1.46) and (1.50) are applicable to all values of $\overline{C}$.

When $\overline{C} > \Gamma^{\mathrm{ap}}$, it is assumed that partitioning process between water and oil only involves monomers. For ionic surfactant the partitioning involves the surfactant molecule and the associated counterion. On the other hand, there is no dissociation in the process of partitioning. $C^{\mathrm{o}}_{\mathrm{mi}}$, $C^{\mathrm{w}}_{\mathrm{mi}}$, and $C^{\mathrm{w}}_{\mathrm{m}}$ are given by the following equation [14]:

$$C^{\mathrm{w}}_{\mathrm{mi}} = f_i \alpha_i \Gamma^{\mathrm{w}}_i \tag{1.52}$$

$$C^{\mathrm{o}}_{\mathrm{mi}} = f_i \alpha_i K_i \Gamma^{\mathrm{w}}_i \tag{1.53}$$

$$C^{\mathrm{w}}_{\mathrm{m}} = \sum C^{\mathrm{w}}_{\mathrm{mi}} \tag{1.54}$$

where f_i is the activity coefficient of surfactant i in a micelle, and it is assumed to be unity. α_i is the molar fraction of surfactant i in mixed micelles and is given by the following equation [14]:

$$\alpha_i = \frac{x_i C_{\mathrm{tol}}}{C_{\mathrm{tol}} - C_{\mathrm{m}}\left(1 + V_{\mathrm{o}}/V_{\mathrm{w}}\right) + f_i \Gamma^{\mathrm{w}}_i + f_i K_i \Gamma^{\mathrm{w}}_i V_{\mathrm{o}}/V_{\mathrm{w}}} \tag{1.55}$$

where C_{m} is the average concentration of total monomeric surfactants in water−oil environments. Summation of the molar fraction of surfactant i in the mixed micelle should be unity and thus [14]:

$$\sum \frac{x_i C_{\mathrm{tol}}}{C_{\mathrm{tol}} - C_{\mathrm{m}}\left(1 + V_{\mathrm{o}}/V_{\mathrm{w}}\right) + f_i \Gamma^{\mathrm{w}}_i + f_i K_i \Gamma^{\mathrm{w}}_i V_{\mathrm{o}}/V_{\mathrm{w}}} = 1 \tag{1.56}$$

For fixed values of other parameters, Eq. (1.56) is a polynomial function of C_{m}. For surfactant mixtures with multiple components, C_{m} has multiple corresponding mathematical values according to the polynomial function of C_{m} defined by Eq. (1.56). However, in reality, C_{m} should only have one value and should be confined in this range:

$$\Gamma^{\mathrm{ap}} < C_{\mathrm{m}} < \overline{C} \tag{1.57}$$

Eqs. (1.56) and (1.57) are solved simultaneously with respect to C_{m}. The apparent cmc of surfactant mixture in water−oil environments is given by the following equation [14]:

$$\Gamma^{\mathrm{ap}} = \frac{1}{\sum \left(x_i/f_i \Gamma^{\mathrm{w}}_i V_{\mathrm{w}}/(V_{\mathrm{w}} + V_{\mathrm{o}}) + f_i K_i \Gamma^{\mathrm{w}}_i V_{\mathrm{o}}/(V_{\mathrm{w}} + V_{\mathrm{o}})\right)} \tag{1.58}$$

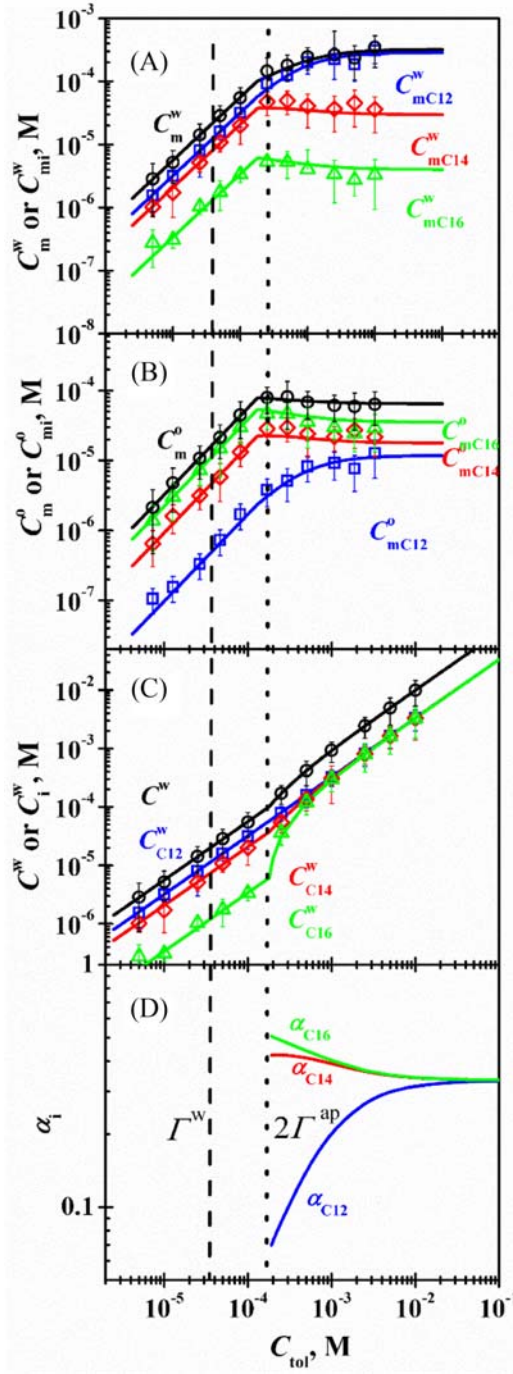

FIGURE 1.16 Properties at equilibrium partitioning of equal-molar mixed BAC surfactants (C_{12}, C_{14}, and C_{16}) in water (0.171 M NaCl)−oil environment at 40°C: (A) concentration of monomeric surfactants in aqueous phase, (B) in oil, (C) concentration of total surfactants in aqueous phase, including monomeric and micellized form, and (D) the composition fraction α_i of surfactant "*i*" in the micelle as a function of initial concentration of total surfactants added to aqueous phase. Symbols: experiment; lines: model prediction. Vertical dash line represents the cmc of surfactant mixture in aqueous phase: Γ^w; vertical dot line represents twice of the apparent cmc of surfactant mixture in water−oil environment: $2\Gamma^{ap}$. *BAC*, Benzalkonium chlorides; *cmc*, critical micelle concentration.

The apparent cmc for pure surfactant i in water−oil environments is given by the following equation [14]:

$$\boldsymbol{\Gamma}_i^{\mathbf{ap}} = \frac{\boldsymbol{K}_i \boldsymbol{\Gamma}_i^{\mathbf{w}} \boldsymbol{V}_{\mathbf{o}} + \boldsymbol{\Gamma}_i^{\mathbf{w}} \boldsymbol{V}_{\mathbf{w}}}{\boldsymbol{x}_i (\boldsymbol{V}_{\mathbf{o}} + \boldsymbol{V}_{\mathbf{w}})} \tag{1.59}$$

This defined apparent cmc of one pure surfactant in water−oil environments can reflect the relative hydrophobicity/hydrophilicity of that surfactant. The higher the apparent cmc of one pure surfactant, the lower the hydrophobicity of that surfactant in water−oil environments. The reverse is also true.

With this developed water/oil surfactant distribution model, the partitioning coefficient K_i of surfactant i, the aqueous cmc of surfactant i, the apparent cmc of mixed surfactants in water−oil environment, Γ^{ap}, monomer concentration of surfactant i in water and oil phases, $C_{\mathrm{mi}}^{\mathrm{w}}$ and $C_{\mathrm{mi}}^{\mathrm{o}}$, and molar fraction of surfactant i in the mixed micelles, α_i, can be predicted in water (containing salts)−oil (nonpolar) at given inputs, which include total surfactant concentration and mixed molar ratio x_i in bulk solution. If experimental data for the cmc and partitioning coefficient of surfactant i are available, it is best to use the experimental data. However, if no experimental data are available, it is best to use the methods introduced previously to predict the aqueous cmc and the partitioning coefficient and then substitute these values into the surfactant distribution model.

The application of water/oil surfactant distribution model to the water−oil partitioning of equal-molar ternary mixtures of BAC surfactants is shown in Fig. 1.16. Fig. 1.16A and B presents equilibrium concentrations of monomeric surfactants in water and in oil versus total initial concentration of mixed surfactants added to the aqueous phase. The intersection of the vertical dashed line and horizontal axis identifies the aqueous cmc of surfactant mixture, which is $\Gamma^{\mathrm{w}} = 3.40 \times 10^{-5}$ M. The partitioning behavior of each mixed surfactant component starts to change as indicated by the transition point in Fig. 1.16A−C. The mixed surfactants form micelles in aqueous phase as indicated by Fig. 1.16C. The preference of the micellar form of C_{16} and C_{14} is reflected by the much higher molar fraction in micelles at the beginning of micelle formation as shown in Fig. 1.16A, indicating the formation of more hydrophobic micelles at the beginning. As the total surfactant concentration increases, the micelles become less hydrophobic.

The application of a water/oil surfactant distribution model is also extended to water−oil partitioning of additional surfactants, as shown in Fig. 1.17A and B for mixed primary alcohol ethoxylates $C_{12}OE_{14}$ and $C_{12}OE_{30}$, Fig. 1.17C and D for mixed hexaoxyethylene nonyl phenyl ether (NPE_6) and octaoxyethylene nonyl phenyl ether (NPE_8), and Fig. 1.17E and F for mixed C_{16} and POE 20 cetyl ether ($C_{16}E_{20}$) in water−oil environments [14]. As can be seen from Fig. 1.17A, the predicted and experimental [121,131] surfactant distribution, as well as the ethoxylate group average per molecule in the oil phase

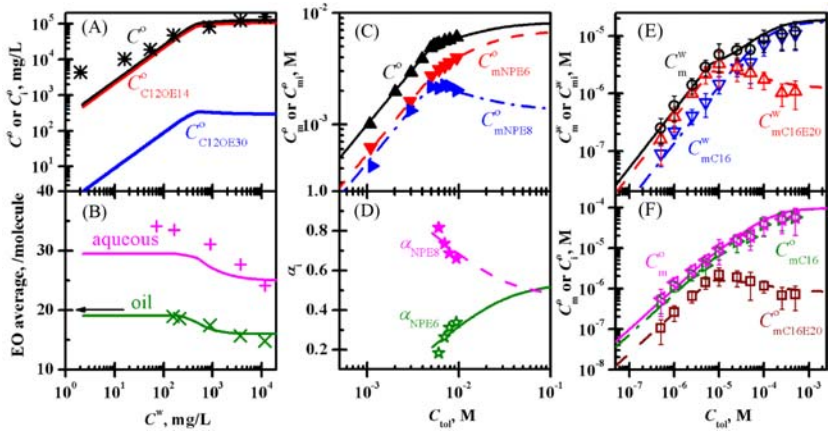

FIGURE 1.17 Comparison between predicted and experimental partitioning properties of surfactants. Parts (A) and (B) are equilibrium partitioning properties of mixed $C_{12}OE_{14}$ and $C_{12}OE_{30}$ surfactants in water−oil (trichloroethylene) environment at 25°C: (A) concentration of surfactants and (B) average EO distribution in aqueous and oil phase as a function of equilibrium aqueous concentration C^w. The values of aqueous cmc are 123.2 and 560 mg/L for $C_{12}OE_{14}$ and $C_{12}OE_{30}$, respectively. Mixed ratio: 0.475/0.525. The arrow in part (B) indicates the initial EO average in water−oil environment. Parts (C) and (D) are equilibrium partitioning properties of mixed NPE_6 and NPE_8 surfactants in water−oil (cyclohexane) environment at 25°C: (C) concentration of monomeric surfactants in oil phase and (D) molar fraction of surfactants in mixed micelles as a function of C_{tol}. The values of aqueous cmc and partitioning coefficients are 2.70×10^{-5} and 4.05×10^{-5} M, and 481 and 70 for NPE_6 and NPE_8, respectively. Mixed ratio: 0.542/0.458. Parts (E) and (F) are equilibrium partitioning properties of mixed C_{16} and $C_{16}E_{20}$ surfactants in water−oil (heptane) environment at 25°C: (E) concentration of monomeric surfactants in 0.03 M NaCl aqueous phase and (F) in oil phase as a function of C_{tol}. The predicted values of aqueous cmc and partitioning coefficients from previous work [71] are 3.61×10^{-5} and 2.47×10^{-6} M, and 5.32 and 0.66 for C_{16} and $C_{16}E_{20}$, respectively. Mixed ratio: 0.542/0.458. Lines: model prediction; symbols: reported data. *cmc*, Critical micelle concentration; *EO*, ethoxylate group.

(trichloroethylene) for mixed $C_{12}OE_{14}$ and $C_{12}OE_{30}$, agree reasonably well. It is interesting to note that when the surfactant distribution model is applied to nonhomologous mixed C_{16} and $C_{16}E_{20}$ in water−oil (heptane) environment, good agreement between experiment and model prediction is observed in Fig. 1.17E and F with respect to the monomer distribution in each phase [14].

This developed WOSDM for the evaluation of the water−oil partitioning of surfactant is applicable over a wide total surfactant concentration range, including the aqueous cmc and the apparent cmc. The model predicted data and the experimental/reported data of surfactant distribution in water−oil environments agree very well. However, the application of this model should be limited to nonpolar or slightly polar organic solvents that do not affect the aqueous cmc significantly as well as to systems in which microemulsion formation is minimized.

15 Surfactant Precipitate and Colloid Formation

Ionic surfactants usually interact with other ions in solution. As surfactants encounter reactive counter ions, they can react to form precipitates. Some surfactants such as carboxylates react with hydrogen ions to form carboxylic acid, which is often in the form of oil droplets. Carboxylates can also react with other positively charged species such as calcium or magnesium ions to form solid, colloidal, hydrophobic particles that behave like microscopic pieces of wax. The process of precipitation to form neutral molecules greatly reduces water solubility. However, the hydrophobic colloidal precipitate particles are often soluble in nonpolar solvents such as oils. Thus precipitation has a very pronounced effect on phase partitioning that strongly favors the lipophilic or oil phase.

Ionic surfactants interact with hydrogen ion, hydroxide ion, and other ions. Consequently, phase stability is often a function of pH [140]. Fig. 1.18 shows the stability regions for oleic acid/sodium oleate in a solution containing calcium ions as noted. Oleate reacts with hydrogen ions to form oleic acid at low pH. The diagram also shows that at high pH and oleate concentrations, aggregate structures form.

The ions Fe^{2+} and Fe^{3+} from iron dissolution can combine with surfactant molecules to form complexes or ligands, which affect the availability of monomeric surfactants in bulk solution and thus compromise adsorption on metal surface. It is also likely that the surfactant adsorption consists of such ligands or complexes that affect the packing efficiency of monolayer/multiplayers. Other components, such as sand, can also compromise the efficiency of surfactants in a way that these components can act as an alternative

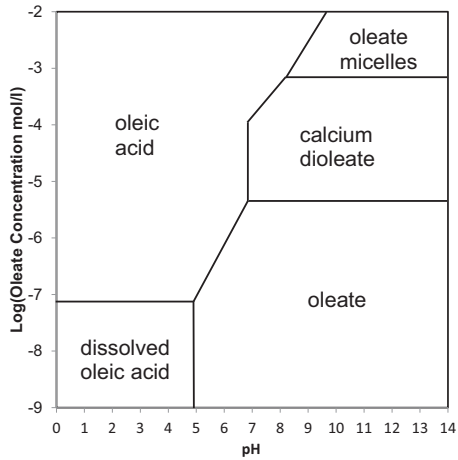

FIGURE 1.18 Comparison of species with respect to total oleate concentration and pH in the presence of 0.0001 M calcium ions.

adsorption sink for the surfactants. Besides the characterization of the specific complex formation processes using experimental techniques, mechanistic models, which are usually based on a combination of the best fit of experimental data and associated theory, may become more useful in a way that the developed model can be extrapolated to similar testing systems, such as the previously mentioned MLA [6]. Note that the quantum chemical methods might be used to evaluate complex formation, but it is challenging to simulate the conditions in realistic WOS environments.

16 Salt/Ion Effects on Surfactant Behavior

The aqueous phase in oil fields generally contains mixtures of various inorganic salts, which not only promote the corrosion of metal in ways as discussed previously, but also affect surfactant-associated processes, including aggregation, adsorption, partitioning, surfactant−ion pair, hydration, and thus affect corrosion inhibition. Any experimental evaluation and modeling work should take this into account. Alternatively, the ion effects on the efficiency of surfactant adsorption may be incorporated into certain processes associated with surfactants, such as aggregation and micellization, which are well accounted for by the abovementioned MLA [6,11] and the WOSDM [14]. At present, these mechanistic modeling methods are well developed to describe the effect of simple 1:1 salt (such as NaCl). More complicated salts [such as $Fe_2(SO_4)_3$] will require additional work so that the model can be tuned for application in more complicated systems with mixtures of salts.

17 Summary

A large quantity of research literature describes the adsorption performance of a wide array of surfactants. Surfactant adsorption is driven by concentration and amphiphilic properties of surfactant as well as surface properties such as charge, defects, and composition. The hydrophilic−hydrophobic nature of surfactants results in interfacial adsorption and aggregation. Surfactants tend to form submonolayer, monolayer/hemimicelle, or bilayer/cylindrical micelle structures at interfaces and surfaces. The concentration needed to achieve monolayer coverage is usually close to the cmc for the surfactant. Aggregation of surfactant above the cmc leads to the formation of spherical micelles and other structures. These structures act like a buffer that maintains the free monomeric surfactant molecule concentration constant when the total surfactant concentration exceeds the level needed for micelle formation. The free monomeric surfactant concentration determines the level of adsorption on a surface. It is possible to predict surfactant adsorption based on material properties, surfactant properties such as hydrocarbon chain length, and solution conditions such as pH and ionic strength.

There are several challenges to more accurate fundamental modeling and predictions of surfactant adsorption, aggregation, and partitioning: (1) the surface state of metals/metal oxides, such as steels, is dynamic and can include different phases as well as metal inclusions and alloying elements that are difficult to incorporate into fundamental modeling. (2) The mechanism of ion/counterion binding to micelle surface and liquid−metal interface is not clear and has been a controversial issue. The ion effects on surface wetting and thus on surface adsorption of surfactants need more study. More complex molecular or multivalent ions such as divalent ions can in principle be modeled as well, but experimental verification and model development are needed. (3) Extensive thermodynamic modeling work on surfactant aggregation and adsorption has been performed, but the research on surfactant adsorption kinetics and surfactant diffusion is limited. Adsorption kinetics and the mass transfer coefficients can be studied through the measurement of equilibrium surface tension and surface tension relaxation profiles at different surfactant concentrations. (4) More experimental work at elevated temperature and higher pressure to more closely simulate field conditions should be performed for additional validation of thermodynamic modeling on surfactant aggregation, adsorption, partitioning, and additional surfactant-associated processes.

Acknowledgment

The work of Y. Zhu was partially performed under the auspices of the US Department of Energy by Lawrence Livermore National Laboratory (LLNL) under Contract DE-AC52-07NA27344.

References

[1] R. Fuchs-Godec, "Effects of Surfactants and their Mixtures on Inhibition of the Corrosion Process of Ferritic Stainless Steel", Electrochim. Acta 54, 2171 (2009).

[2] Y. Tang, L. Yao, C. Kong, W. Yang and Y. Chen, "Molecular Dynamics Simulations of Dodecylamine Adsorption on Iron Surfaces in Aqueous Solution", Corros. Sci. 53, 2046 (2011).

[3] B. Kronberg, "Surfactant Mixtures", Curr. Opin. Colloid Interface Sci. 2, 456 (1997).

[4] M. L. Free, "A New Corrosion Inhibition Model for Surfactants that more Closely Accounts for Actual Adsorption than Traditional Models that Assume Physical Coverage is Proportional to Inhibition", Corros. Sci. 46, 3101 (2004).

[5] M. L. Free, "Understanding the Effect of Surfactant Aggregation on Corrosion Inhibition of Mild Steel in Acidic Medium", Corros. Sci. 44, 2865 (2002).

[6] Y. Zhu, M. L. Free and G. Yi, "Electrochemical Measurement, Modeling, and Prediction of Corrosion Inhibition Efficiency of Ternary Mixtures of Homologous Surfactants in Salt Solution", Corros. Sci. 98, 417 (2015).

[7] K. Videm and A. Dugstad, "Corrosion of Carbon Steel in an Aqueous Carbon Dioxide Environment. Part 1. Solution Effects", Mater. Perform. 28, 63 (1989).

[8] B. Mishra, S. Al-Hassan, D. Olson and M. Salama, "Development of a Predictive Model for Activation-Controlled Corrosion of Steel in Solutions Containing Carbon Dioxide", Corrosion 53, 852 (1997).

[9] J. O'M Bockris and A. K. N. Reddy, *Modern Electrochemistry*, 2nd Edition, Plenum Press, New York, NY (2000).

[10] O. L. Riggs Jr, "Theoretical Aspects of Corrosion Inhibitors and Inhibition", in: *Corrosion Inhibitors*, C. C. Nathan (Ed.), National Association of Corrosion Engineers (NACE), Houston, TX (1973), pp. 7−27.

[11] Y. Zhu, M. L. Free and G. Yi, "The Effects of Surfactant Concentration, Adsorption, Aggregation, and Solution Conditions on Steel Corrosion Inhibition and Associated Modeling in Aqueous Media", Corros. Sci. 102, 233 (2016).

[12] G. Gece, "Drugs: A Review of Promising Novel Corrosion Inhibitors", Corros. Sci. 53, 3873 (2011).

[13] Y. Zhu, M. L. Free and G. Yi, "Experimental Investigation and Modeling of the Performance of Pure and Mixed Surfactant Inhibitors: Aggregation, Adsorption, and Corrosion Inhibition on Steel Pipe in Aqueous Phase", J. Electrochem. Soc. 162, C582 (2015).

[14] Y. Zhu and M. L. Free, "Experimental Investigation and Modeling of the Performance of Pure and Mixed Surfactant Inhibitors: Partitioning and Distribution in Water-Oil Environments", J. Electrochem. Soc. 162, C702 (2015).

[15] M. L. Free, W. Wang and D. Y. Ryu, "Prediction of Corrosion Inhibition Using Surfactants", Corrosion 60, 837 (2004).

[16] W. Wang and M. L. Free, "Prediction and Measurement of Corrosion Inhibition of Mild Steel Using Nonionic Surfactants in Chloride Media", Corros. Sci. 46, 2601 (2004).

[17] R. C. Pasquali, N. Sacco and C. Bregni, "The Studies on Hydrophilic-Lipophilic Balance (HLB): Sixty Years after William C. Griffin's Pioneer Work (1949−2009)", Latin Am. J. Pharmacy 28, 313 (2009).

[18] M. E. Aulton, *Pharmaceutics: The Design and Manufacture of Medicines*, 2nd Edition, Churchill Livingstone Imprint, Elsevier, Oxford, UK (2003).

[19] B. A. Wills, *Mineral Processing Technology. An Introduction to the Practical Aspects of Ore Treatment and Mineral Recovery*, 3rd Edition, Pergamon Imprint, Elsevier, Oxford, UK (1985).

[20] D. Y. Ryu and M. L. Free, "Use of Electrochemical Noise Measurements for Determining the Rate of Corrosion and the Surfactant Aggregate Transition Concentration at the Mild Steel−Liquid Interface", Adsorp. Sci. Technol. 22, 155 (2004).

[21] D. A. Jones, *Principles and Prevention of Corrosion*, Macmillan Publishing Company, London, UK (1992).

[22] M. Migahed, M. Hegazy and A. Al-Sabagh, "Synergistic Inhibition Effect Between Cu^{2+} and Cationic Gemini Surfactant on the Corrosion of Downhole Tubing Steel During Secondary Oil Recovery of Old Wells", Corros. Sci. 61, 10 (2012).

[23] W. Durnie, R. De Marco, A. Jefferson and B. Kinsella, "Development of a Structure−Activity Relationship for Oil Field Corrosion Inhibitors", J. Electrochem. Soc. 146, 1751 (1999).

[24] C. D. Taylor, A. Chandra, J. Vera and N. Sridhar, "A Multiphysics Perspective on Mechanistic Models for Chemical Corrosion Inhibitor Performance", J. Electrochem. Soc. 162, C369 (2015).

[25] M. Christov and A. Popova, "Adsorption Characteristics of Corrosion Inhibitors from Corrosion Rate Measurements", Corros. Sci. 46, 1613 (2004).

[26] P. C. Okafor and Y. Zheng, "Synergistic Inhibition Behaviour of Methylbenzyl Quaternary Imidazoline Derivative and Iodide Ions on Mild Steel in H_2SO_4 Solutions", Corros. Sci. 51, 850 (2009).

[27] X. Shi, R. Q. Zhang, C. Minot, K. Hermann, M. A. Van Hove, W. Wang and N. Lin, "Complex Molecules on a Flat Metal Surface: Large Distortions Induced by Chemisorption can make Physisorption Energetically More Favorable", J. Phys. Chem. Lett. 1, 2974 (2010).
[28] J. N. Israelachvili, *Intermolecular and Surface Forces*, 3rd Edition, Academic Press Imprint, Elsevier, Oxford, UK (2011).
[29] S. D. Stoyanov, V. N. Paunov, H. Rehage and H. Kuhn, "A New Class of Interfacial Tension Isotherms for Nonionic Surfactants Based on Local Self-Consistent Mean Field Theory: Classical Isotherms Revisited", Phys. Chem. Chem. Phys. 6, 596 (2004).
[30] D. S. Valkovska, G. C. Shearman, C. D. Bain, R. C. Darton and J. Eastoe, "Adsorption of Ionic Surfactants at an Expanding Air−Water Interface", Langmuir 20, 4436 (2004).
[31] A. M. Díez-Pascual, A. Compostizo, A. Crespo-Colín, R. G. Rubio and R. Miller, "Adsorption of Water-Soluble Polymers with Surfactant Character: Adsorption Kinetics and Equilibrium Properties", J. Colloid Interface Sci. 307, 398 (2007).
[32] M. Szpakowska, A. Magnuszewska and O. B. Nagy, "Mechanism of Nitromethane Liquid Membrane Oscillator Containing Sodium Oleate", J. Colloid Interface Sci. 325, 494 (2008).
[33] A. Frumkin and B. Damaskin, "Adsorption of Organic Substances on the Free Water Surface and at the Water−Mercury Interface", Pure Appl. Chem. 15, 263 (1967).
[34] Q. Zhou and M. Rosen, "Molecular Interactions of Surfactants in Mixed Monolayers at the Air/Aqueous Solution Interface and in Mixed Micelles in Aqueous Media: The Regular Solution Approach", Langmuir 19, 4555 (2003).
[35] R. Atkin, V. S. Craig, E. J. Wanless and S. Biggs, "Mechanism of Cationic Surfactant Adsorption at the Solid−Aqueous Interface", Adv. Colloid Interface Sci. 103, 219 (2003).
[36] V. Schram and S. B. Hall, "Thermodynamic Effects of the Hydrophobic Surfactant Proteins on the Early Adsorption of Pulmonary Surfactant", Biophys. J. 81, 1536 (2001).
[37] M. L. Free and J. D. Miller, "Kinetics of 18-Carbon Carboxylate Adsorption at the Fluorite Surface", Langmuir 13, 4377 (1997).
[38] R. Mortimer, Chapter 6: Multicomponent Systems, *Physical Chemistry*, The Benjamin-Cummings Publishing Company, Academic Press Imprint, Elsevier, Oxford, UK (1993), pp. 203−260.
[39] H.-J. Butt, K. Graf and M. Kappl, *Physics and Chemistry of Interfaces*, 3rd Edition, Wiley-VCH, John Wiley and Sons, Hoboken, NJ (2013).
[40] R. J. Hunter, *Foundations of Colloid Science*, 2nd Edition, Oxford University Press, Oxford, UK (2001).
[41] K. Shinoda, M. Hato and T. Hayashi, "Physicochemical Properties of Aqueous Solutions of Fluorinated Surfactants", J. Phys. Chem. 76, 909 (1972).
[42] S. Ozeki, M.-A. Tsunoda and S. Ikeda, "Surface Tension of Aqueous Solutions of Dodecyldimethylammonium Chloride, and its Adsorption on Aqueous Surfaces", J. Colloid Interface Sci. 64, 28 (1978).
[43] J. Goodwin, *Colloids and Interfaces with Surfactants and Polymers*, 2nd Edition, John Wiley and Sons, Hoboken, NJ (2009).
[44] J. Drelich, The Role of Wetting Phenomena in the Hot Water Process for Bitumen Recovery from Tar Sand, Ph.D. Dissertation, The University of Utah, Salt Lake City, UT (1993).
[45] E. G. Kelly and D. J. Spottiswood, *Introduction to Mineral Processing*, John Wiley and Sons, Somerset, NJ (1982).
[46] A. Carré and K. L. Mittal (Eds.), Superhydrophobic Surfaces, CRC Press, Boca Raton, FL (2009).

[47] B. Deraguin and L. Landau, "Theory of the Stability of Strongly Charged Lyophobic Sols and of the Adhesion of Strongly Charged Particles in Solution of Electrolytes", Acta Physicochim. USSR 14, 633 (1941).
[48] E. D. Shchukin, A. V. Pertsov, E. A. Amelina and A. S. Zelenev, Colloid and Surface Chemistry, Volume 12, Elsevier, Oxford, UK (2001).
[49] P. Atkins, *Physical Chemistry. Equilibrium Electrochemistry: Ions and Electrodes*, 3rd Edition, Oxford University Press, Oxford, UK (1986), pp. 237–245.
[50] K. W. Kolasinski, *Surface Science: Foundations of Catalysis and Nanoscience*, John Wiley and Sons, Hoboken, NJ (2012).
[51] L. L. Schramm, *Emulsions, Foams, and Suspensions: Fundamentals and Applications*, Wiley-VCH, Weinheim, Germany (2005).
[52] M. Kodama and S. Seki, "Thermodynamical Investigations on Phase Transitions of Surfactant-Water Systems: Thermodynamic Stability of Gel and Coagel Phases and the Role of Water Molecules in their Appearance", Adv. Colloid Interface Sci. 35, 1 (1991).
[53] A. I. Rusanov, *Micellization in Surfactant Solutions*, Harwood Academic Publishers, Reading, UK (1997).
[54] S. Oh and D. O. Shah, "The Effect of Micellar Lifetime on the Rate of Solubilization and Detergency in Sodium Dodecyl Sulfate Solutions", J. Am. Oil Chem. Soc. 70, 673 (1993).
[55] C. Tanford, *The Hydrophobic Effect: Formation of Micelles and Biological Membranes*, 2nd Edition, John Wiley and Sons, Somerset, NJ (1980).
[56] S. V. Koroleva and A. I. Victorov, "Modeling of the Effects of Ion Specificity on the Onset and Growth of Ionic Micelles in a Solution of Simple Salts", Langmuir 30, 3387 (2014).
[57] B. Jönsson, B. Lindman, K. Holmberg and B. Kronberg, Chapter 2: Surfactant Micellization, in: *Surfactants and Polymers in Aqueous Solution*, John Wiley and Sons, Chichester, UK (1998), pp. 3–60.
[58] K. Shinoda, *Principles of Solution and Solubility*, Marcel Dekker, New York, NY (1978).
[59] V. Chhabra, M. L. Free, P. K. Kang, S. E. Truesdail and D. O. Shah, "Microemulsions as an Emerging Technology: From Petroleum Recovery to Nanoparticle Synthesis of Magnetic Materials and Superconductors", Tenside Surfact. Deterg. 34, 156 (1997).
[60] R. Nagarajan and E. Ruckenstein, "Molecular Theory of Microemulsions", Langmuir 16, 6400 (2000).
[61] R. M. Hill, "Applications of Surfactant Mixtures", in: *Mixed Surfactant Systems*, K. Ogino and M. Abe (Eds.), Marcel Dekker, New York (1993), pp. 317–336.
[62] M. J. Rosen, *Surfactants and Interfacial Phenomena*, 3rd Edition, Wiley-Interscience, John Wiley and Sons, Hoboken, NJ (2004).
[63] P. C. Okafor, C. Liu, X. Liu and Y. Zheng, "Inhibition of CO_2 Corrosion of N8o Carbon Steel by Carboxylic Quaternary Imidazoline and Halide Ions Additives", J. Appl. Electrochem. 39, 2535 (2009).
[64] E. Oguzie, Y. Li and F. Wang, "Corrosion Inhibition and Adsorption Behavior of Methionine on Mild Steel in Sulfuric Acid and Synergistic Effect of Iodide Ion", J. Colloid Interface Sci. 310, 90 (2007).
[65] M. Heydar and M. Javidi, "Corrosion Inhibition and Adsorption Behaviour of an Amido-Imidazoline Derivative on API 5L X52 Steel in CO_2-Saturated Solution and Synergistic Effect of Iodide Ions", Corros. Sci. 61, 148 (2012).
[66] S. Y. Shiao, A. Patist, M. L. Free, V. Chhabra, P. D. T. Huibers, A. Gregory, S. Patel and D. O. Shah, "The Importance of Sub-Angstrom Distances in Mixed Surfactant Systems for Technological Processes", Colloids Surf. A 128, 197 (1997).

[67] S. Y. Shiao, V. Chhabra, A. Patist, M. L. Free, P. D. T. Huibers, A. Gregory, S. Patel and D. O. Shah, "Chain Length Compatibility Effects in Mixed Surfactant Systems for Technological Applications", Adv. Colloid Interface Sci. 74, 1 (1998).

[68] R. Zhang and P. Somasundaran, "Advances in Adsorption of Surfactants and Their Mixtures at Solid/Solution Interfaces", Adv. Colloid Interface Sci. 123, 213 (2006).

[69] P. Somasundaran and S. Krishnakumar, "Adsorption of Surfactants and Polymers at the Solid-Liquid Interface", Colloids Surf. A 123, 491 (1997).

[70] Y. Zhu, M. L. Free and J.-H. Cho, "Integrated Evaluation of Mixed Surfactant Distribution in Water-Oil-Steel Pipe Environments and Associated Corrosion Inhibition Efficiency", Corros. Sci. 110, 213 (2016).

[71] Y. Zhu, M. L. Free, R. Woollam and W. Durnie, "A Review of Surfactants as Corrosion Inhibitors and Associated Modeling", Prog. Mater. Sci. 90, 159 (2017).

[72] W. W. Focke, N. S. Nhlapo and E. Vuorinen, "Thermal Analysis and FTIR Studies of Volatile Corrosion Inhibitor Model Systems", Corros. Sci. 77, 88 (2013).

[73] M. Knag, J. Sjöblom, G. Øye and E. Gulbrandsen, "A Quartz Crystal Microbalance Study of the Adsorption of Quaternary Ammonium Derivates on Iron and Cementite", Colloids Surf. A 250, 269 (2004).

[74] C. Gabler, C. Tomastik, J. Brenner, L. Pisarova, N. Doerr and G. Allmaier, "Corrosion Properties of Ammonium Based Ionic Liquids Evaluated by SEM-EDX, XPS and ICP-OES", Green Chem. 13, 2869 (2011).

[75] A. Kokalj, S. Peljhan, M. Finsgar and I. Milošev, "What Determines the Inhibition Effectiveness of ATA, BTAH, and BTAOH Corrosion Inhibitors on Copper?" J. Am. Chem. Soc. 132, 16657 (2010).

[76] I. B. Obot, D. D. Macdonald and Z. M. Gasem, "Density Functional Theory (DFT) as a Powerful Tool for Designing New Organic Corrosion Inhibitors. Part 1: An Overview", Corros. Sci. 99, 1 (2015).

[77] A. Kokalj, M. Lozinšsek, B. Kapun, P. Taheri, S. Neupane, P. Losada-Pérez, C. Xie, S. Stavber, D. Crespo, F. U. Renner, A. Mol and I. Milošev, "Simplistic Correlations Between Molecular Electronic Properties and Inhibition Efficiencies: Do They Really Exist?" Corros. Sci. 179, 108856 (2020).

[78] C. Feiler, D. Mei, B. Vaghefinazari, T. Würger, R. H. Meißner, B. J. C. Luthringer-Feyerabend, D. A. Winkler, M. L. Zheludkevich and S. V. Lamaka, "*In Silico* Screening of Modulators of Magnesium Dissolution", Corros. Sci. 163, 108245 (2020).

[79] T. L. P. Galvaõ, G. Novell-Leruth, A. Kuznetsova, J. O. Tedim and J. R. B. Gomes, "Elucidating Structure−Property Relationships in Aluminum Alloy Corrosion Inhibitors by Machine Learning", J. Phys. Chem. C 124, 5624 (2020).

[80] S. Zhang, Z. Tao, S. Liao and F. Wu, "Substitutional Adsorption Isotherms and Corrosion Inhibitive Properties of Some Oxadiazol-Triazole Derivative in Acidic Solution", Corros. Sci. 52, 3126 (2010).

[81] E. Naderi, A. Jafari, M. Ehteshamzadeh and M. Hosseini, "Effect of Carbon Steel Microstructures and Molecular Structure of Two New Schiff Base Compounds on Inhibition Performance in 1 M HCl Solution by EIS", Mater. Chem. Phys. 115, 852 (2009).

[82] P. C. Hiemenz and R. Rajagopalan, *Principles of Colloid and Surface Chemistry*, 3rd Edition, Marcel Dekker, New York, NY (1997).

[83] S. Nešić, "Key Issues Related to Modelling of Internal Corrosion of Oil and Gas Pipelines—A Review", Corros. Sci. 49, 4308 (2007).

[84] C. Aharoni and M. Ungarish, "Kinetics of Activated Chemisorption. Part 2—Theoretical Models", J. Chem. Soc. Faraday Trans. 1 (73), 456 (1977).

[85] A. Adamson and A. Gast, *Physical Chemistry of Surfaces*, 6th Edition, John Wiley and Sons, Hoboken, NJ (1997).

[86] R. Fuchs-Godec and M. G. Pavlović, "Synergistic Effect Between Non-Ionic Surfactant and Halide Ions in the Forms of Inorganic or Organic Salts for the Corrosion Inhibition of Stainless-Steel X4Cr13 in Sulphuric Acid", Corros. Sci. 58, 192 (2012).

[87] D. G. Brown and K. S. Al Nuaimi, "Nonionic Surfactant Sorption onto the Bacterial Cell Surface: A Multi-Interaction Isotherm", Langmuir 21, 11368 (2005).

[88] K. Birdi, *Introduction to Electrical Interfacial Phenomena*, CRC Press, Taylor and Francis Group, Boca Raton, FL (2010).

[89] Y. Zhu, Integrated Modeling of Mixed Surfactants Distribution and Corrosion Inhibition Performance in Oil Pipelines, Ph.D. Dissertation, The University of Utah, Salt Lake City, UT (2015).

[90] S. Ramachandran, C. Menendez, V. Jovancicevic and J. Long, "Film Persistency of New High-Temperature Water-Based Batch Corrosion Inhibitors for Oil and Gas Wells", J. Petrol. Explor. Prod. Technol. 2, 125 (2012).

[91] R. De Marco, W. Durnie, A. Jefferson, B. Kinsella and A. Crawford, "Persistence of Carbon Dioxide Corrosion Inhibitors", Corrosion 58, 354 (2002).

[92] A. K. Singh, S. K. Shukla, M. Singh and M. A. Quraishi, "Inhibitive Effect of Ceftazidime on Corrosion of Mild Steel in Hydrochloric Acid Solution", Mater. Chem. Phys. 129, 68 (2011).

[93] W.-H. Jang and J. D. Miller, "Molecular Orientation of Langmuir-Blodgett and Self-Assembled Monolayers of Stearate Species at a Fluorite Surface as Described by Linear Dichroism Theory", J. Phys. Chem. 99, 10272 (1995).

[94] M. L. Free, 18-Carbon Unsaturated Carboxylate Adsorption Phenomena at the Fluorite Surface, Ph.D. Dissertation, The University of Utah, Salt Lake City, UT (1994).

[95] S. H. Chen and C. W. Frank, "Infrared and Fluorescence Spectroscopic Studies of Self-Assembled *n*-Alkanoic Acid Monolayers", Langmuir 5, 978 (1989).

[96] Y. Zhu and M. L. Free, "Experimental Investigation and Modeling of the Performance of Pure and Mixed Surfactant Inhibitors: Micellization and Corrosion Inhibition", Colloids Surf. A 489, 407 (2016).

[97] Y. Zhu and M. L. Free, "Evaluation of Ion Effects on Surfactant Aggregation from Improved Molecular Thermodynamic Modeling", Indus. Eng. Chem. Res. 54, 9052 (2015).

[98] A. Goldsipe and D. Blankschtein, "Modeling Counterion Binding in Ionic − Nonionic and Ionic − Zwitterionic Binary Surfactant Mixtures", Langmuir 21, 9850 (2005).

[99] F. S. Lima, I. M. Cuccovia, D. Horinek, L. Q. Amaral, K. A. Riske, S. Schreier, R. K. Salinas, E. L. Bastos, P. A. R. Pires, J. C. Bozelli Jr, D. C. Favaro, A. C. B. Rodrigues, L. G. Dias, O. A. El Seoud and H. Chaimovich, "Effect of Counterions on the Shape, Hydration, and Degree of Order at the Interface of Cationic Micelles: The Triflate Case", Langmuir 29, 4193 (2013).

[100] F. S. Lima, F. A. Maximiano, I. M. Cuccovia and H. Chaimovich, "Surface Activity of the Triflate Ion at the Air/Water Interface and Properties of *N,N,N*-Trimethyl-*N*-Dodecylammonium Triflate Aqueous Solutions", Langmuir 27, 4319 (2011).

[101] C. Oelschlaeger, P. Suwita and N. Willenbacher, "Effect of Counterion Binding Efficiency on Structure and Dynamics of Wormlike Micelles", Langmuir 26, 7045 (2010).

[102] R. R. Netz and D. Horinek, "Progress in Modeling of Ion Effects at the Vapor/Water Interface", Annu. Rev. Phys. Chem. 63, 401 (2012).
[103] S. V. Koroleva and A. I. Victorov, "The Strong Specific Effect of Coions on Micellar Growth from Molecular-Thermodynamic Theory", Phys. Chem. Chem. Phys. 16, 17422 (2014).
[104] L. Moreira and A. Firoozabadi, "Molecular Thermodynamic Modeling of Specific Ion Effects on Micellization of Ionic Surfactants", Langmuir 26, 15177 (2010).
[105] M. N. Jones and J. Piercy, "Light Scattering Studies on *N*-Dodecyltrimethylammonium Bromide and *N*-Dodecylpyridinium Iodide", J. Chem. Soc. Faraday Trans. 1 (68), 1839 (1972).
[106] S. Ozeki and S. Ikeda, "The Sphere-Rod Transition of Micelles of Dodecyldimethylammonium Bromide in Aqueous NaBr Solutions, and the Effects of Counterion Binding on the Micelle Size, Shape and Structure", Colloid Polym. Sci. 262, 409 (1984).
[107] T. Imae, R. Kamiya and S. Ikeda, "Formation of Spherical and Rod-Like Micelles of Cetyltrimethylammonium Bromide in Aqueous NaBr Solutions", J. Colloid Interface Sci. 108, 215 (1985).
[108] T. Imae and S. Ikeda, "Sphere-Rod Transition of Micelles of Tetradecyltrimethylammonium Halides in Aqueous Sodium Halide Solutions and Flexibility and Entanglement of Long Rodlike Micelles", J. Phys. Chem. 90, 5216 (1986).
[109] H. Nomura, S. Koda, T. Matsuoka, T. Hiyama, R. Shibata and S. Kato, "Study of Salt Effects on the Micelle−Monomer Exchange Process Of Octyl-, Decyl-, and Dodecyltrimethylammonium Bromide in Aqueous Solutions by Means of Ultrasonic Relaxation Spectroscopy", J. Colloid Interface Sci. 230, 22 (2000).
[110] L. J. Magid, Z. Han, Z. Li and P. D. Butler, "Tuning Microstructure of Cationic Micelles on Multiple Length Scales: The Role of Electrostatics and Specific Ion Binding", Langmuir 16, 149 (2000).
[111] J. H. Clint, "Micellization of Mixed Nonionic Surface Active Agents", J. Chem. Soc. Faraday Trans. 1 (71), 1327 (1975).
[112] P. M. Holland and D. N. Rubingh, "Nonideal Multicomponent Mixed Micelle Model", J. Phys. Chem. 87, 1984 (1983).
[113] K. S. Pitzer, *Activity Coefficients in Electrolyte Solutions*, CRC Press, Taylor and Francis Group, Boca Raton, FL (2018).
[114] J. N. Butler, *Ionic Equilibrium: Solubility and pH Calculations*, John Wiley and Sons, Hoboken, NJ (1998).
[115] B. Lukanov and A. Firoozabadi, "Specific Ion Effects on the Self-Assembly of Ionic Surfactants: A Molecular Thermodynamic Theory of Micellization with Dispersion Forces", Langmuir 30, 6373 (2014).
[116] U. P. Preiss, P. Eiden, J. Łuczak and C. Jungnickel, "Modeling the Iinfluence of Salts on the Critical Micelle Concentration of Ionic Surfactants", J. Colloid Interface Sci. 412, 13 (2013).
[117] G. Barnes and I. Gentle, *Interfacial Science: An Introduction*, 2nd Edition, Oxford University Press, Oxford, UK (2011).
[118] S. Endo and K.-U. Goss, "Predicting Partition Coefficients of Polyfluorinated and Organosilicon Compounds using Polyparameter Linear Free Energy Relationships (PP-LFERs)", Environ. Sci. Technol. 48, 2776 (2014).
[119] A. Graciaa, J. Andérez, C. Bracho, J. Lachaise, J. L. Salager, L. Tolosa and F. Ysambertt, "The Selective Partitioning of the Oligomers of Polyethoxylated Surfactant Mixtures Between Interface and Oil and Water Bulk Phases", Adv. Colloid Interface Sci. 123, 63 (2006).

[120] E. H. Crook, D. B. Fordyce and G. F. Trebbi, "Molecular Weight Distribution of Nonionic Surfactants: II. Partition Coefficients of Normal Distribution and Homogeneous *p, t*-Octylphenoxyethoxy-ethanols (OPEs)", J. Colloid Sci. 20, 191 (1965).

[121] T. C. B. Kibbey and L. Chen, "Phase Volume Effects in the Sub- and Super-CMC Partitioning of Nonionic Surfactant Mixtures Between Water and Immiscible Organic Liquids", Colloids Surf. A 326, 73 (2008).

[122] J. L. Salager, N. Márquez, A. Graciaa and J. Lachaise, "Partitioning of Ethoxylated Octylphenol Surfactants in Microemulsion − Oil − Water Systems: Influence of Temperature and Relation Between Partitioning Coefficient and Physicochemical Formulation", Langmuir 16, 5534 (2000).

[123] J. G. Del Rio, D. G. Hayes and V. S. Urban, "Partitioning Behavior of an Acid-Cleavable, 1,3-Dioxolane Alkyl Ethoxylate, Surfactant in Single and Binary Surfactant Mixtures for 2- and 3-Phase Microemulsion Systems According to Ethoxylate Head Group Size", J. Colloid Interface Sci. 352, 424 (2010).

[124] B. W. Brooks and H. N. Richmond, "The Application of a Mixed Nonionic Surfactant Theory to Transitional Emulsion Phase Inversion: 1. Derivation of a Mixed Surfactant Partitioning Model", J. Colloid Interface Sci. 162, 59 (1994).

[125] B. W. Brooks and H. N. Richmond, "The Application of a Mixed Nonionic Surfactant Theory to Transitional Emulsion Phase Inversion: 2. The Relationship Between Surfactant Partitioning and Transitional Inversion—A Thermodynamic Treatment", J. Colloid Interface Sci. 162, 67 (1994).

[126] J. L. Salager, N. Márquez, R. E. Antón, A. Graciaa and J. Lachaise, "Retrograde Transition in the Phase Behavior of Surfactant−Oil−Water Systems Produced by an Alcohol Scan", Langmuir 11, 37 (1995).

[127] F. Ravera, M. Ferrari, L. Liggieri, R. Miller and A. Passerone, "Measurement of the Partition Coefficient of Surfactants in Water/Oil Systems", Langmuir 13, 4817 (1997).

[128] M. Ben Ghoulam, N. Moatadid, A. Graciaa and J. Lachaise, "Effects of Oxyethylene Chain Length and Temperature on Partitioning of Homogeneous Polyoxyethylene Nonionic Surfactants Between Water and Isooctane", Langmuir 18, 4367 (2002).

[129] Y. Zhu, V. Molinier, M. Durand, A. Lavergne and J.-M. Aubry, "Amphiphilic Properties of Hydrotropes Derived from Isosorbide: Endo/Exo Isomeric Effects and Temperature Dependence", Langmuir 25, 13419 (2009).

[130] A. Van de Voorde, C. Lorgeoux, M.-C. Gromaire and G. Chebbo, "Analysis of Quaternary Ammonium Compounds In Urban Stormwater Samples", Environ. Pollut. 164, 150 (2012).

[131] M. A. Cowell, T. C. B. Kibbey, J. B. Zimmerman and K. F. Hayes, "Partitioning of Ethoxylated Nonionic Surfactants in Water/NAPL Systems: Effects of Surfactant and NAPL Properties", Environ. Sci. Technol. 34, 1583 (2000).

[132] A. Graciaa, J. Lachaise, J. Sayous, P. Grenier, S. Yiv, R. Schechter and W. Wade, "The Partitioning of Complex Surfactant Mixtures Between Oil/Water/Microemulsion Phases at High Surfactant Concentrations", J. Colloid Interface Sci 93, 474 (1983).

[133] M. Balcan and D. F. Anghel, "The Partition of Ethoxylated Non-Ionic Surfactants Between Two Non-Miscible Phases", Colloid Polym. Sci. 283, 982 (2005).

[134] R. Aveyard, B. P. Binks, S. Clark and P. D. I. Fletcher, "Effects of Temperature on the Partitioning and Adsorption of $C_{12}E_5$ in Heptane−Water Mixtures", J. Chem. Soc. Faraday Trans. 86, 3111 (1990).

[135] R. Aveyard, B. P. Binks, S. Clark and J. Mead, "Interfacial Tension Minima in Oil−Water−Surfactant Systems. Behaviour of Alkane−Aqueous NaCl Systems Containing Aerosol OT", J. Chem. Soc. Faraday Trans. 1 (82), 125 (1986).

[136] R. Tadmouri, C. Zedde, C. Routaboul, J.-C. Micheau and V. Pimienta, "Partition and Water/Oil Adsorption of Some Surfactants", J. Phys. Chem. B 112, 12318 (2008).

[137] A. V. Marenich, C. J. Cramer and D. G. Truhlar, "Universal Solvation Model Based on Solute Electron Density and on a Continuum Model of the Solvent Defined by the Bulk Dielectric Constant and Atomic Surface Tensions", J. Phys. Chem. B 113, 6378 (2009).

[138] G. Scalmani and M. J. Frisch, "Continuous Surface Charge Polarizable Continuum Models of Solvation. I. General Formalism", J. Chem. Phys. 132, 114110 (2010).

[139] S. H. Yalkowsky, Y. He and P. Jain, *Handbook of Aqueous Solubility Data*, 2nd Edition, CRC Press, Taylor and Francis Group, Boca Raton, FL (2019). Copyright 2010.

[140] M. L. Free and J. D. Miller, "The Significance of Collector Colloid Adsorption Phenomena in the Fluorite/Oleate Flotation System as Revealed by FTIR/IRS and Solution Chemistry Analysis", Intl. J. Miner. Process. 48, 197 (1996).

This page intentionally left blank